

NAL PROPOSAL NO. 206

Correspondent: V. Z. Peterson  
Department of Physics  
and Astronomy  
University of Hawaii  
Honolulu, Hawaii 96822

FTS/Off-net:

808-948-7925

DEVELOPMENT OF A TRANSITION RADIATION DETECTOR  
FOR DISCRIMINATING BETWEEN PIONS AND KAONS  
AT NAL ENERGIES

F. Harris, T. Katsura, S. Parker, V. Peterson,  
and V. Stenger

University of Hawaii

R. Ellsworth, G. B. Yodh

University of Maryland

S. Pruss

National Accelerator Laboratory

March 12, 1973

*Harris - ?*

## SUMMARY OF PROPOSAL

### Development of a Transition-Radiation Detector for Particle Identification at NAL Energies

Development of a transition-radiation detector (TR detector) for use at NAL as a particle identifier in a bubble-chamber beam is proposed as a joint university-NAL project. The principal advantage of the TR-detector is that the TR-signal and particle discrimination increase with momentum, whereas in conventional methods (e.g., relativistic rise in ionization, gas Cerenkov counters) particle discrimination becomes extremely difficult at high gamma ( $\gamma = E/m$ ). In the overlap region between gas Cerenkov and TR (100 - 400 GeV/c), it is shown that the two methods complement each other, since Cerenkov more readily identifies mesons ( $\pi/K$ ) from protons while TR more readily identifies (pions) from (K/p). It is proposed to make a direct experimental comparison between the present NAL gas Cerenkov in the beamline to the 30-inch bubble chamber and a "phase I" TR-detector in the same beamline.

The "phase I" NAL TR-detector would utilize a single radiator of 1000 thin Be foils just before a bending magnet (enclosure 112) in order to separate the TR photon signal from beam-charged particles. TR-detection by a multi-celled xenon MWPC located well downstream (enclosure 114) at the end of a long vacuum pipe is designed to discriminate strongly against backgrounds of high energy photons. The estimated detected TR-signal from 400 GeV

## NAL TR Proposal - Summary

pions is 5.2 photons in the 5 to 50 KeV range with total energy of 94 KeV; kaons of 400 GeV/c would produce only 7.0% of this yield, and protons even less. Simple pulse-height discrimination should accept pions with 96% efficiency and reject 96% of kaons.

The above predictions are based on projections of experimental results obtained by the Hawaii-Maryland-Oxford collaboration in TR-runs with electron and pion beams at the Bevatron and at SLAC over the 1 to 15 GeV/c range. MWPC detectors filled with argon, krypton, and xenon were used in the true proportional mode, yielding absolute pulse-height distributions from each of 8 to 11 chambers. Examples of both "sandwich array" and "magnetic separation" array results are compared with theory, and the limitations of the technique are considered. The resulting "phase I" TR-detector is a relatively simple improvement upon the existing H-M-O TR-detector and data-handling system.

"Phase II" of TR-development would seek to detect coherent TR-production from many equally spaced foils, not only as a physics experiment but also to improve mass discrimination. Theoretically, the TR is emitted in hollow cones whose angles depend upon  $\gamma$  and TR-photon energy; if the photon "pattern" (and energy of each photon) are measured, then particle  $\gamma$  (and mass) definition is improved. The Hawaii group's experience with delay-line readout of MWPC indicates that both position and ionization can be read out simultaneously with

NAL TR Proposal - Summary

sufficient accuracy. NAL offers the first chance to observe coherent TR, since multiple scattering of electrons in the foil radiator destroys coherence; however, 400 GeV pions in 1000 1-mil Be foils will be fully coherent.

OUTLINE

- I. Introduction
- II. Basic Proposal: Phase I
  - Experimental Arrangement
  - Yields of Photon and X-Ray Energy
  - Pion vs. (Kaon/Proton) Discrimination
  - Backgrounds in the "Magnetic-Separation" Array
- III. Transition Radiation: Theory and Experiment
  - Summary of Basic Theory
  - Foil Radiators
  - TR-X-Ray Detectors: MWPC and Solid-State Detectors
  - Radiator-Detector Arrays
    - "Sandwich" Array
    - "Magnetic-Separation" Array
  - Experimental Results with Electrons
  - Yuan, et al., Other References
  - H-M-0 Bevatron Results
  - H-M-0 SLAC Results
- IV. Complementary Role of Gas Cerenkov and Transition-Radiation Detector in Identifying High-Momentum Particles
  - Comparison of Particle Identification Between TRD and Gas Cerenkov in Bubble-Chamber Beamline
  - Improvements in Gas Cerenkov Counters and Transition-Radiation Detectors

## NAL TR Proposal

### V. Details of the Phase I NAL TR-Detector

Beryllium Foil Radiator

Secondary Electrons Produced by Kaons in Be Foils

Xenon MWPC Detector

Data-Handling System; On-Line Computer

Tagging for the 30-Inch Bubble Chamber

### VI. Coherent Transition Radiation; Phase II TR-Detector

Angular Distribution of Coherent TR

Multiple Scattering in the Foils

Energy and Position Detection with Delay-Line Readout  
of MWPC

### VII. Schedule, Personnel, and Budget

Time Schedule

Personnel

Budget

### References

### Figures

Enclosure A: Preprint of NI&M on Bevatron TR-Experiment  
(H-M-O Group)

Enclosure B: "Transition Radiation," by S. I. Parker  
(XVI International Conference on High Energy  
Physics)

## I. INTRODUCTION

Particle identification becomes progressively more difficult as particle energies greatly exceed their rest masses; i.e., as they become ultrarelativistic. NAL at 400 GeV already provides particles with gammas ( $\gamma = E/m$ ) ranging from several hundreds to several thousands; a 400 GeV pion has  $\gamma = 2860$ . Momentum can be measured with considerable accuracy by magnetic deflection. However, the established methods of determining mass by combining momentum with measurement of a velocity-dependent property (e.g., relativistic rise of ionization loss) become less sensitive as gamma increases. Relativistic rise in gases (argon, krypton, or xenon) reaches a plateau at  $\gamma \approx 1000$ , and 90% of this increase in ionization occurs by  $\gamma \approx 500$  (only 70 GeV for pions). The difference in ionization between pions and kaons of 400 GeV is less than 3%. Thus ionization measurements are of little use for particle discrimination at NAL.

Much more hopeful are prospects for further refinements in the already highly developed design of gas Cerenkov counters (e.g., the DISC counter).<sup>(1)</sup> Such counters detect velocity differences as small as  $\Delta\beta \approx 10^{-6}$ . Kaons and pions of 400 GeV have  $\Delta\beta = 5 \times 10^{-7}$ . Thus it is pressing the already highly refined "state of the art" of gas Cerenkovs to expect clear-cut identification of pions from kaons at 400 GeV. (In order to achieve this feat, it will be necessary to continuously

monitor the index of refraction to several parts in  $10^8$  and correct for variations!) Furthermore, the particles identified must be severely collimated in order to maintain detection efficiency. Thus, despite remarkable improvements in the precision of gas Cerenkov counters over the past decade or so, it seems likely that their performance as particle identifiers will not be able to keep pace with accelerator energies of 400, 500, and perhaps 1000 GeV in the foreseeable future.

Clearly, a detector whose response is sensitive to  $\gamma \simeq p/m$  would be most useful as a particle identifier, <sup>particularly</sup> if the detection efficiency was close to 100%. Transition Radiation (or "TR") provides the basis for such a detector.

TR from a single interface is linearly dependent upon gamma,

$$W_{\gamma}(\text{single interface}) = \frac{1}{3}\alpha \cdot \hbar\omega_p \cdot \gamma, \quad (1)$$

where  $\alpha = 1/137$  is the fine structure constant, and  $\omega_p$  is the plasma frequency of the dielectric ( $\hbar\omega_p = 24.4$  eV for Mylar). A vacuum-dielectric interface is assumed. Although the absolute yield per interface is small, the yield increases with particle energy and many foils can be used. (Interference effects lead to saturation in yield for any given array, but proper design can maximize the gamma-dependence for a given range.) Practical NAL arrays with 400 GeV pions should yield ~6 detected photons well separated from known backgrounds. In Section II, we show that kaons (and protons) produce an

order-of-magnitude fewer photons than pions. Thus the prospects for a useful TR-detector at NAL seem good.

The original concept of "Transition Radiation" is due to Frank and Ginzburg;<sup>(2)</sup> this radiation from a dielectric boundary is related to, but not the same as, Cerenkov radiation (TR has no threshold velocity). Alikhanian<sup>(3)</sup> first investigated transition radiation experimentally and he foresaw its potential application as a relativistic particle detector. The theory has been developed to a high degree, largely by Garibian<sup>(4)</sup> and associates. Experimentally, the most extensive work in the U.S.A. or Europe has been done by Luke Yuan and colleagues over the past 5 years or so, initially with optical radiation<sup>(5)</sup> and more recently with X-rays.<sup>(6)</sup>

Our interest in TR is more recent and rather directly connected with other preparations for NAL experiments (the "EMI" project or Experiment 155 plus an earlier development of MWPC to detect  $\pi^0$ -photons by a "proportional quantameter"). The Hawaii-developed proportional chambers and readout system were readily adapted to TR X-ray detection by filling the MWPC with krypton or xenon. Multi-module MWPCs interleaved with Mylar foil radiators were used. A brief Bevatron run in July 1971<sup>(7)</sup> showed strong TR-signals for electrons with  $\gamma \approx 6000$ . Improved equipment and a wider range of electron energies at SLAC (August 1972) provided much more extensive data.<sup>(8)</sup> Detailed comparison of these data with theory have

given us confidence that we can predict accurately the TR yield from pions, kaons, and protons at NAL.

Several of the Hawaii personnel involved in the EMI development (Harris, <sup>BAENZIG</sup> Peterson, Stenger) are also involved in this proposal. The Maryland and Oxford personnel listed here were also actively involved in both the Bevatron and SLAC runs, and will join in this proposal to the extent outlined in Section VII. We have also sought NAL collaboration, especially as an overlap with the gas Cerenkov counter team. Much of the equipment already exists and could be assembled rather quickly, if approval and adequate support are given.

A very interesting "physics" problem (described by W.K.H. Panofsky as "fun and games with Maxwell's equations") is the detection of coherent transition radiation from many equally spaced foils. Theory predicts energy and angular peaking (see Section VI). Our electron-produced TR was not expected to show coherence since multiple scattering of electrons would mask the effect. However, NAL pions of 400 GeV are ideal for producing coherent TR. When Phase I succeeds, we plan to proceed to Phase II which involves adding position readout to the MWPC detectors.

The following sections detail various aspects of the Proposal.

## II. BASIC PROPOSAL: PHASE I

The basic proposal is to develop and install a single TR-detector for 100 - 400 GeV pions in the beamline to the 30-inch bubble chamber. The TR-detector output would be compared with that of the present gas Cerenkov counter on a particle-by-particle basis. This is "Phase I" of our TR Proposal.

The TR-detector should work most effectively at the highest momenta (e.g., 400 GeV), but it is possible that it will still be useful in discriminating pions from (kaons/protons) at momenta as low as 100 GeV. Thus we hope to overlap the useful region for Cerenkov discrimination. Since TR effectively discriminates pions from (kaons/protons), while the Cerenkov most readily distinguishes (pions/kaons) from protons, the combined Cerenkov-TR signals may prove to be an effective Kaon-signature.

Phase I involves only "straightforward" extension of the techniques and equipment already used successfully in our Bevatron and SLAC runs. This included the "magnetic separation" method, sealed-off xenon MWPC X-ray detectors, and a multi-channel ADC-computer data acquisition system. The only innovations are the use of Be foils as radiators, the first use of fast pions to radiate TR, and a new multi-compartment xenon MWPC. The expected TR photon yields and energy spectrum, detector efficiency, and pulse-height distribution are interpolated from our own experimental results

and are consistent with theoretical estimates.

Experimental Arrangement. Figure 1-a is a schematic diagram of the proposed experimental arrangement: the 1000-foil radiator is located upstream of the horizontal bending magnet pair in Enclosure 112. Thus TR radiation produced will be well separated from the charged-particle beam at Enclosure 114, where X-rays would be detected by a thick (20 cm) xenon-filled MWPC chamber. The entire flight path for TR would be in vacuum; we propose a 16-inch vacuum pipe in place of the present 8-inch pipe. The spatial separation between pion and TR beam at Enclosure 114 will be 18 cm, whereas both beam spots will be about 5 cm in diameter.

Figure 1-b is a copy of a portion of an NAL scale drawing (unnumbered) which shows the locations of the enclosures, Cerenkov, and magnets. The charged-particle beam is bent 3.4 milliradians horizontally and 3.4 milliradians vertically (up) by 4 magnets in Enclosure 112. The beam size at the entrance to the first magnet is about  $1\frac{1}{2}$ " in diameter (measured), although calculations predict that it can be focused to smaller size. We have chosen our foil size to be 2" x 2" to adequately cover the beam.

The foil radiator assembly would consist of 1000 1-mil Be foils spaced 0.030" apart. It would be best to mount the radiator assembly in vacuum in order to reduce X-ray absorption; approximately 16% of the otherwise detectable flux is absorbed in 30 inches of air. The foil radiator is a "passive" element,

which needs only (remote?) mechanical motion for operation; an "equivalent absorber" (1.00" Be = 4.7 gm/cm<sup>2</sup>) to replace the radiator assembly for background runs is also required.

The xenon MWPC detector downstream would be mounted in air at the end of the 16-inch vacuum pipe. The xenon MWPC would consist of ten (10) 2-cm compartments--each in principle a separate MWPC--within a common gas barrier. Each compartment is read out separately, and the energy-detection pattern provides a "signature" for TR-X-rays; this discriminates strongly against backgrounds such as charged particles and high-energy photons. In addition, an anti-counter placed behind the MWPC rejects events accompanied by penetrating radiation. (Both methods were used successfully in our SLAC "MS" array runs.)

The data-acquisition equipment (ADC, CAMAC electronics, on-line computer, etc.) would be located nearby the xenon MWPC. (See Section V.)

Yields of Photon and X-ray Energy. Since the TR photon yields are low ( $\sim \alpha$  per interface), every effort must be made to use as many interfaces as possible. At the same time, the "formation zone" requirements (see Section II) of minimum foil thickness and plasma frequency set a lower limit on material in the beam. Self-absorption of X-rays in the foil material strongly suppresses low-energy X-rays. Low-Z material is obviously desirable; we have used Mylar and polyethylene and now propose to use Beryllium ( $\rho = 1.83$ ,  $\hbar\omega_p = 25.8$  eV).

Figure 2 shows the "radiator yields" of TR photons and total X-ray energy emerging from the bottom of a stack of N-foils of .001" Be, per incident 400 GeV pion. The inter-foil spacing is .030" of vacuum. The total photon cross-section (sum of photoelectric, coherent, and incoherent scattering) is used for self-absorption. The yields begin to saturate at about 1000 foils of Be. (The improvement of Be over Mylar is clear: to obtain the same yield from 0.001" Mylar, we would have to have five separate radiators of 188 foils each!) (See Section V.)

The angular distribution of TR from many regularly spaced foils is complicated since it involves coherent effects (see Section VI). However, for purposes of detector geometry, it is sufficient to note that almost all TR energy emerging from the radiator will be contained in a cone whose half angle is  $\theta \approx 1/\gamma$ . Thus pions of 400 GeV/c in Enclosure 112 will produce TR whose "intrinsic spot size" at the detector in Enclosure 114 will be about 3.7 cm in diameter.

The average detection efficiency  $\langle \epsilon \rangle$  of the thick xenon MWPC is quite high for TR-X-rays: 64% of the energy and 74% of the photons emerging from the Be-radiator will be detected. (See Section V for details.) At the same time, the gas proportional counter is "thin" to high-energy photons, charged particles, and other probable background sources.

The predicted single-photon spectra of detected TR from 400 GeV/c pions and kaons are shown in Figure 3: (a) the

single-photon pulse-height distribution with energy,  $dN/dE$ -vs- $E$ , where  $E = h\omega$  is the energy of an individual photon, and (b) the energy spectra  $dW/dE$ -vs- $E$  for individually detected TR-photons, where  $\frac{dW}{dE} = E \cdot \frac{dN}{dE}$ . The broad peaks are due to single-foil interference effects. (The experimental resolution has not been folded in.) These curves are basic to predicting the yield and mass resolution of the TR-detector. Note that 400 GeV/c kaons yield much less TR-energy than 400 GeV/c pions.

The variation with momentum of the average total detected TR-energy,

$$W_D = \int \epsilon(E) \frac{dW}{dE} dE, \quad (2)$$

is shown in Figure 4-~~a~~<sup>b</sup> for pions and kaons. The uncertainty in the values plotted are primarily statistical fluctuations due to the limited number of photons detected. Due to the very low TR from kaons at these momenta, the ratio of  $\pi/K$  TR signal is 15:1--implying strong discrimination between pions and (kaons/protons).

The number of TR-photons detected from pions and kaons is plotted as a function of particle momentum in Figure 4-~~b~~<sup>a</sup>. The average number of TR-photons from 400 GeV/c pions is 5.2; this number is comparable to the number of photoelectrons detected in gas Cerenkov counters. Using Poisson statistics, we can calculate the efficiency of the TR-counter for detecting at least one TR-photon,

$$\epsilon(\geq 1) = 1 - e^{-\langle N \rangle},$$

as 99.5% for 400 GeV/c pions.

Pion vs. (Kaon/Proton) Discrimination. The primary measure of discrimination between  $\pi$  and (K/p) is the total pulse height from the TR-detector, although the "signature" (distribution of detected TR-energy among the cells of the xenon MWPC) may further enhance the discrimination. The total pulse height is readily used for on-line electronic decisions. "Signature" decisions are best reserved to off-line computer analyses; this will be quite practical in bubble-chamber experiments.

The predicted total pulse-height distributions for 400 GeV/c pions and kaons are shown in Figure for the Phase I TR-detector. These resolution curves are derived from the single-photon distributions of Figure 3, taking into account the statistical fluctuations of the number of photons detected per event as well as the energy per photon. A Monte Carlo technique was used. The resolution between  $\pi$  and K is readily apparent, especially at 400 GeV/c. One can identify pions with 96% efficiency by simple pulse-height discrimination by setting the discrimination level at 30 KeV. Only 4% of kaons would count.

The Phase I TR-detector would be employed primarily to "tag" pions in the presence of protons and kaons. The combination of gas Cerenkov signal from ( $\pi$  or K) plus TR-signal from  $\pi$  only offers the possibility of clearcut tagging of both  $\pi$  and K at these "intermediate" momenta. At higher momenta where the K TR-signal is greater, the TR-detector

might tag positively both  $\pi$  and K on pulse height alone.

Backgrounds in the "Magnetic-Separation" Array. The principal backgrounds encountered in the SLAC runs were (a) charged particles, (b) bremsstrahlung in the foils and other beamline material, and (c) unknown sources of electromagnetic radiation. These backgrounds were measured by running with an "equivalent absorber" (single foil equivalent to total radiator thickness) which produced negligible TR.

The background of collimated charged particles was effectively eliminated at SLAC by either using an anti-counter behind the X-ray detector or by discarding events showing dE/dx ionization pulses in all eight chambers in line.

The non-charged particle backgrounds measured at SLAC ranged from 0.2 to 0.5 KeV per 1.5 cm of xenon. (See Section III.) This background was uniformly distributed between chambers; i.e., it was much more penetrating than the X-rays. About half of this background could be accounted for by bremsstrahlung produced by electrons in the radiator material and 20-meter long helium bag. (SLAC is also a well-known "sea" of e.m. radiation!)

The NAL backgrounds should be somewhat different. The general "sea" of electromagnetic radiation should be lower than at SLAC. NAL pions will produce much less bremsstrahlung than SLAC electrons. A vacuum path for TR will avoid absorbing X-rays. The long distance will permit magnetic sweeping of stray-charged particles produced by pions or

protons in the  $4.7 \text{ gm/cm}^2$  of Beryllium radiator. Thus we expect lower background, as well as higher signal at NAL in comparison with SLAC.

## III. TRANSITION RADIATION: THEORY AND EXPERIMENT

This section contains a very brief summary of useful theoretical formulae plus a comparison of our own experimental results (Hawaii-Maryland-Oxford, or "H-M-O" group) with predictions. Our basic purpose is to establish beyond question that Transition Radiation can be observed with relatively simple equipment and that theoretical estimates can be relied upon to predict the TR-signal in the new regime of NAL pion/kaon/proton beams.

Summary of Basic Theory. The differential distribution of TR-energy from a fast-charged particle of velocity  $\beta c$  traversing a single dielectric interface ( $\epsilon_1 \rightarrow \epsilon_2$ ) is<sup>(4)</sup>

$$\frac{d^2W}{d\Omega dE} = \frac{\alpha\beta^2}{\pi} \sin^2\theta \cos^2\theta \times \left| \frac{(\epsilon_1 - \epsilon_2)(1 - \beta^2 - \beta \sqrt{\epsilon_1 - \epsilon_2} \sin^2\theta)}{(1 - \beta^2 \epsilon_2 \cos^2\theta)(\epsilon_1 \cos\theta + \sqrt{\epsilon_2} \sqrt{\epsilon_1 - \epsilon_2} \sin^2\theta)(1 - \beta \sqrt{\epsilon_1 - \epsilon_2} \sin^2\theta)} \right|^2, \quad (3)$$

where  $E = \hbar\omega$  is the photon energy and  $\epsilon_i$  are dielectric constants. For ultrarelativistic particles and considering X-ray energies ( $\epsilon_i = 1 - \xi_i^2$ ),

$$\frac{d^2W}{d\Omega dE} = \frac{\alpha\theta^2}{\pi^2} \left| \frac{1}{\gamma^{-2} + \theta^2 + \xi_1^2} - \frac{1}{\gamma^{-2} + \theta^2 + \xi_2^2} \right|^2, \quad (4)$$

where  $\xi_i = \omega_{ip}/\omega$  and  $\omega_{ip} = \sqrt{\frac{4\pi n_i e^2}{m_e}} \approx 29 \sqrt{Z/A}$  is the plasma frequency of the dielectric. If  $\xi_1^2 = 0$  (vacuum) and  $\xi_2^2 \ll 1$ ,

we can integrate over solid angle to obtain the energy spectrum,

$$\frac{dW}{dE} \sim \frac{\alpha}{\pi} \left[ \frac{(2 + \xi^2 \gamma^2)}{\xi^2 \gamma^2} \ln(1 + \xi^2 \gamma^2) - 2 \right]. \quad (5)$$

Further integration over photon energy yields

$$W_1 = \frac{1}{3} \alpha \cdot \kappa_{\omega_p} \cdot \gamma. \quad (1)$$

The above formulae are for a single interface.

When a foil is used in vacuum, there are two interfaces involved, generating TR field amplitudes with intrinsic phase differences of  $180^\circ$  (rare-dense vs. dense-rare transitions).

Interference between amplitudes from the front and back surfaces of the foil introduces a strong dependence upon the phase shift ( $a_f$ ) between the front and back. Too thin a foil produces almost complete cancellation. Thus the foil thickness ( $t$ ) must provide a phase difference for the amplitudes to add constructively. The yield varies  $\sim \sin^2 \frac{1}{2} a_f$ , where  $a = t/z$  and  $z$  is a "characteristic length" (or formation zone). This "formation zone" is a function of gamma,  $E = \kappa\omega$ , and emission angle  $\theta$ , and is given approximately by:

$$Z(\gamma, \omega, \theta) \approx \frac{2c}{\omega} \cdot \left\{ \gamma^{-2 + \xi^2 + \theta^2} \right\}^{-1}. \quad (6)$$

$Z_f$  for polyethylene has a value of 0.4 mils for  $\gamma = 5870$ ,  $\kappa\omega = 10$  KeV, and  $\theta = 1/\gamma = 0.38$  milliradians. Figure 6 shows the variation of  $Z$  with X-ray energy in polyethylene ( $\kappa_{\omega_p} = 20.0$  eV) and in air for various gamma. Note that at low photon energies, the formation zone thickness is insensitive to gamma.

The distribution in energy and angle of TR produced by the addition of radiation from a series of regularly spaced foils of thickness  $t_f$  and spacing between foils of  $t_g$ , neglecting self-absorption, is

$$\frac{d^2W}{dE \cdot d\theta} \approx \frac{\alpha}{2\pi} \theta^3 \left(\frac{\omega}{c}\right)^4 Z_f^2 Z_g^2 \sin^2 \frac{a_f}{2} \cdot \left(\frac{\sin \frac{N\phi}{2}}{\sin \frac{\phi}{2}}\right)^2, \quad (7)$$

where  $Z_f$  = formation zone in the foil,  $Z_g$  = formation zone in vacuum ( $\omega_p = 0$ ),  $a_f = t_f/Z_f$  is the phase shift per foil, and  $\phi = a_f + a_g$ . The last term (the "diffraction-grating" term) rapidly oscillates as a function of X-ray energy and angle and is strongly peaked at certain angles for a given frequency. Such effects may be observable with NAL pions (see Section VI); however with electrons, the angular effects are "washed out" (due to multiple scattering) and the average value ( $N$ ) is used. Thus the incoherent yield for  $N$  foil-gap modules is just  $N$  times the single-module yield.

Integration of (7) over angle is quite complicated, and we have done it numerically in a computer program which also incorporates absorption in the foils, the response of the detector, multiple scattering, and other effects. However, the general result is that the average energy increases with  $\gamma$ , but less than linearly.

The single-photon energy spectrum of TR emission is shown

in Figure 7 for  $\gamma = 5870$  (3.0 GeV electrons), both for a single interface and for the specific case of 100 2-mil foils for polyethylene (20.0 eV) spaced .125" apart in air. The strong self-absorption of softer X-rays within the Mylar foils produces the "radiator yield" attenuated at low energies. As a practical matter, the many interfaces and minimum foil thickness required always result in strong self-absorption of photons below about 3 to 4 KeV. Thus the TR-flux incident upon the MWPC detector will be above 4 KeV. The "upper limit" on the TR-spectrum occurs at about  $k\omega_{lim} \approx \frac{1}{2}(k\omega_p)\gamma$ , which is 72 KeV for  $\gamma = 5870$ . Thus for  $5 < k < 72$  KeV, we seek efficient detection of TR-photons. A xenon gas proportional chamber (or 8 thin MWPC in series) makes an efficient detector (49% of the XTR detected). The bottom curve in Figure 7 shows the detected energy spectrum of single photons.

Foil Radiators. The basic requirement of a TR-foil material is that it must have a high electron density; i.e., high plasma frequency. Table I lists the plasma energies of some widely used (or considered) TR-radiator materials. A second requirement is that foil thickness must be comparable (or greater than) the "formation zone" for the frequency, particle velocity, and angle considered; some typical values of Z (for  $\gamma = 2860$ ,  $E = 10$  KeV, and  $\theta = 1/\gamma$ ) are tabulated. Finally, the attenuation of TR-X-rays by absorption in successive foils limits the number of foils which can be usefully utilized in a radiator assembly. If the geometrical acceptance of the detector is

large, the attenuating processes include not only the photoelectric effect but also coherent and incoherent scattering. Table I lists the mean absorption distance ( $\lambda$ ) at 10 KeV. Also listed is the "maximum number of foils" ( $N_{\max}$ ), which is defined as the limiting value of

$$N_{\text{eff.}} = I_N/I_1 = \frac{1-e^{-Nt/\lambda}}{1-e^{-t/\lambda}} \xrightarrow{N \rightarrow \infty} (1-e^{-t/\lambda})^{-1} = N_{\max},$$

where  $N$  = true number of foils. Thus  $N_{\max} \cdot I_1 = I_{\infty}$  is the limiting TR-intensity from an "infinite" multi-foil array, relative to single-foil intensity.

Table I  
TR-Radiator Foil Characteristics\*

$$\gamma = 2860, E = 10 \text{ KeV}$$

Material	$K_{\omega p}$ (e.V. <sup>p</sup> )	Z (mils)	$\lambda$ (cm)	$N_{\max}$ (.001")
Be	25.8	0.23	0.923	363
Polyethylene	20.0	0.36	0.49	192
Mylar	24.4	0.25	0.188	74
Al	33.0	0.14	0.015	6

\*J. D. Bateman<sup>(9)</sup> has proposed "deuterium foam" as a low-Z radiator.

Due to self-absorption, the number of foils in a radiator is limited to approximately  $N_{\max}$  at the mean X-ray energy of interest. Additional TR-energy can be obtained only by

employing repeated radiator-detector arrays; e.g., the "sandwich" array. The yield per array is roughly proportional to  $N_{\max}$ , but the actual number of foils used is typically  $N \approx 1.6 N_{\max}$ , which yields 80% of  $N_{\max}$  intensity.

TR-X-Ray Detectors: MWPC and Solid-State Detectors. This is also discussed briefly in Enclosure B. Both solid-state counters and gas-filled MWPC have been used successfully<sup>(6,7,8)</sup> in detecting TR in the X-ray region. Consideration of background from charged particles and high-energy photons argues for using detectors which are "thin" to background and "thick" to TR X-rays. A relatively large area ( $100 \text{ cm}^2$ ) may be required. It is often useful to employ several layers of detector in order to measure the absorption properties of the signal; i.e., obtain the "signature" of the event. For these reasons, we have concentrated on the development of noble-gas MWPC. However, in cases where very good energy resolution is desired (see Section VI) solid-state counters may be needed.

We have developed<sup>(8)</sup> sealed-off MWPC filled with xenon (or krypton, or argon) which maintain constant pulse height and energy resolution (21%) over several days between flushing. This drastically reduces the cost of xenon and krypton.

As shown in Figure 7, the typical energy spectrum of XTR emerging from a radiator is peaked at about 15 KeV, and the intensity falls to 1% of peak at the lower limit of 3 KeV and the higher limit of 180 KeV. This is a good match to photoelectric absorption of krypton and xenon; the K-edges

are 14.3 KeV (krypton) and 34.6 KeV (xenon). Figure 8 is a plot of the "energy-detection efficiency,  $\epsilon_w$ ," of our 1.5 cm thick MWPC as filled with argon, krypton, or xenon. The average detection efficiencies for the "stack" spectrum of Figure 7 are 2.7% (argon), 12% (krypton), and 16% (xenon). The calculated efficiency includes photoelectric absorption of TR X-rays in the gas, escape or reabsorption of fluorescent photons, and the Auger effect; but we have not yet corrected for the escape of long-range electrons from a 1.5 cm thick chamber.

(In the NAL experiments, we propose a much thicker chamber, 20 cm of xenon, which will reduce range escape and fluorescent escape to negligible levels. See Section V).

Radiator-Detector Arrays. In order to detect several photons/particle, an "array" of radiator-detector "modules" is often used. At least two types of "arrays" are useful:

- (1) The "sandwich" array, in which the charged particle passes directly through a number of foil-and-detector modules placed in line;
- (2) the "magnetic-separation" array, in which magnetic deflection after the foil radiator is used to achieve spatial separation of the charged particle from the TR-photons.

These two arrays are represented schematically in Figure 9.

The "sandwich" array provides a compact arrangement with low foil self-absorption and N-fold sampling of both particle dE/dx and TR-spectra. The SW-array suffers from the fact that

the Landau fluctuations in collision energy-loss are inextricably mixed with detected TR-photons in the total pulse-height spectrum. The total array thickness ( $\text{gm/cm}^2$ ) to the charged-particle beam may also create problems.

The "magnetic-separation" method has the advantage that it yields directly the TR-photon spectrum if backgrounds are low. In the MS-method, foil self-absorption limits the total photon yield. Also, electrons will produce synchrotron radiation during magnetic deflection.

The ultimate resolution in  $\gamma$  (and thus in mass) depends primarily upon the statistics of the number of TR-photons detected. For a given  $\gamma$ -resolution, the SW-array requires more TR-photons than the MS-array since "unfolding" of TR from Landau is required.

(We have chosen the MS-array for the Phase I NAL setup since the photon yield is adequate for good  $\pi$ -vs-K,p resolution and the TR "signature" is clearcut.)

Experimental Results with Electrons. The most comprehensive data on MWPC detection of TR have been obtained by Yuan, et al.<sup>(6)</sup> and in two recent experiments<sup>(7,8)</sup> which the Hawaii-Maryland-Oxford collaboration has conducted. Since we are most familiar with our own experiments, we will illustrate this section with our own data.

Enclosure A describes our Bevatron "sandwich" array runs using argon- and krypton-filled MWPC, 100  $\frac{1}{2}$ -mil Mylar foils, and electrons of 1.3 GeV/c ( $\gamma = 2550$ ) and 3.0 GeV/c ( $\gamma = 5870$ ).

Figure 7 of Enclosure A reproduces the pulse-height spectra from krypton MWPC using 3.0 GeV/c pions and electrons (with and without radiator). The 11-chamber summed signal shows a well defined "TR-shift." The "radiator-in" peak is a factor of 1.42 times the electron Landau peak, an absolute shift of 36.4 KeV (3.3 KeV/chamber). An average of at least  $5.0 \pm 0.5$  TR-photons per electron was detected by the array. The Landau peak (dE/dx only) was 25 KeV (FWHM); the "radiator-in" peak increased to 42 KeV (FWHM) due to combined Landau fluctuations and TR-photon energy fluctuations. We have not attempted to derive the experimental TR-spectrum from these data, but the average shift (36.4 KeV) agrees with predictions for these detectors.

A more extensive experimental investigation was carried out at SLAC during August 1972, using a new 16-channel ADC and CAMAC computer on-line readout. The MWPC detectors were improved so that they could be run sealed-off for long periods without degradation in pulse height or energy resolution; this enabled us to use xenon as well as krypton and argon for long runs. The SLAC beam provided electrons and pions at 3, 6, 9, 12, and 15 GeV with good energy definition and low intensity. The "sandwich" array was used with 8 chambers. A new "magnetic-separation" array, involving a 20-meter long, 250-gauss bending magnet, was used successfully to separate the electrons from the TR-photons; the MWPC were "split" electrically into two halves, and the TR side absorbed photons while the electron

side measured  $dE/dx$ . Eight (8) xenon-filled chambers in line were read out separately, using our 16-channel ADC. A shower counter was used to identify the electron and fix its position for valid events.

The "sandwich" array (SW) SLAC runs were qualitatively similar to the Bevatron data but over a wider energy range with better equipment, better statistics, and better calibration. Mylar foils of  $\frac{1}{2}$ -mil and 1-mil thicknesses were used. The MWPC were run with argon and then with krypton fillings. A partial summary of the results with 1-mil Mylar (100 foils, 100 mils apart) and krypton detector (8x1.5 cm MWPC) is given in Table II:

Table II  
SLAC Sandwich-Array Runs with Electrons  
(Mylar (100, 1, 100); Krypton (8 PC)

Electron Energy	Total Ionization Energy			
	Photons Detected	Radiators	E. A.*	Net TR
3 GeV	3.48±.09	156 KeV	98.8 KeV	57.2 KeV
9 GeV	4.62	202 KeV	116.8 KeV	85.2 KeV
15 GeV	4.86	206 KeV	110.0 KeV	104.0 KeV

\*E. A. = "Equivalent absorber" (0.100" Mylar slab/chamber)  $dE/dx$  collision loss, plus background, in 8 chambers.

(These are preliminary data, lacking detailed calibration corrections; hence ionization energy may be in error by  $\pm 10\%$ , although the number of photons should be reliable.) Note that

the number of photons increases more slowly than the net TR-energy; i.e., the average X-ray energy increases. Figure 10 shows the predicted yield of TR-energy and photons detected by 1.5 cm krypton, as a function of gamma. The MWPC detection efficiency has been folded in. The initial linear increase turns into a logarithmic dependence at high gamma, as expected from Equation (5), for this foil thickness. (Fortunately, the NAL gammas are in the linear range!) The agreement between theory and experiment is reasonable, considering the present uncertainty ( $\sim 20\%$ ) in the experimental corrections.

The "E. A." pulse-height distributions are typical Landau distributions; this provides additional energy calibration. Subtraction of E. A. runs from "radiator-in" runs corrects for most backgrounds; these are small in comparison to  $dE/dx$ . The average TR-energy  $\langle W \rangle$  is obtained by straight subtraction:  $\langle W \rangle = \langle W + \Delta \rangle - \langle \Delta \rangle$ , where  $\langle \Delta \rangle$  is the mean  $\frac{dE}{dx}$  value. The TR-energy spectrum, however, can be obtained only <sup>by</sup> "unfolding." The number of "TR-photons detected" obtained by straight subtraction is a lower limit, subject to corrections due to two photons detected in one chamber. (These corrections have not yet been made.)

A new feature of the SLAC run is the "magnetic-separation" (MS) array data, which was run entirely with xenon MWPC detectors. This run was made primarily to test the feasibility of deflecting the electron "gently" (to keep synchrotron radiation low) by only 5 to 8 cm and still record both the  $dE/dx$  signal and TR

X-rays in electrically-separated halves of the same MWPC. (This system worked well, although a small correction for induced signal is required.) Two factors limited the total signal in these runs: (1) only one radiator could be used, and the total thickness was limited by self-absorption to about 0.2" polyethylene and (2) the 8 thin (1.5 cm) xenon MWPC did not constitute the optimum detector (a single, much thicker, chamber of xenon would be more efficient since fluorescent escape photons are especially important in xenon). Nevertheless, we obtained signals well above background, with only 0.5 TR-photons/electron detected. (The results can be extrapolated to 5-10 photons/electron, using Be-foils and a thick xenon detector.)

Figure 11 provides a sample of the preliminary data from the MS array for 3.0 GeV electrons radiating from 100 polyethylene foils (2-mils thick, 125-mils spacing). The 8 xenon MWPC outputs are summed in (a) to provide an overall pulse-height distribution; since the average number of detected photons is less than one, Figure 11-a is essentially a "single-photon distribution." A theoretical calculation of the spectrum of detected energy is also shown; the average detected energy was predicted to be 19.4 KeV.

A "signature" of TR-X-rays is provided by their attenuation within ~10 cm of xenon gas. Backgrounds from charged particles or high-energy photons will behave much differently. Figure 11-b shows the measured variation in average energy

(per electron) among the 8 MWPC in-line.. Using such "a priori" distributions, a  $\chi^2$  or maximum likelihood fit of unknown events can be made to improve particle identification and background rejection.

As can be seen from the above, both the Sandwich array and Magnetic-Separation array results from the SLAC run are understood. We feel that we can confidently predict the TR-signal to be expected in the NAL Phase I array.

IV. COMPLEMENTARY ROLE OF GAS CERENKOV AND TRANSITION-RADIATION  
DETECTOR IN IDENTIFYING HIGH-MOMENTUM PARTICLES

The gas Cerenkov counter is a velocity selector whose velocity resolution,  $\Delta\beta$ , is defined in terms of the range of Cerenkov angle,  $\Delta\theta$ , accepted by the counter:

$$\Delta\beta = \tan \theta \cdot \Delta\theta .$$

Kinematically, this is related to the momentum  $p$  of two particles of different masses  $m_0$  and  $m_1$  by:

$$\Delta\beta = \frac{(m_1^2 - m_0^2)}{2p^2} .$$

The kinematic separation between pions and kaons at 300 GeV/c is  $\Delta\beta \approx 10^{-6}$ . The ratio  $\Delta\beta(\pi K) = 0.35 \Delta\beta(Kp)$  for the same  $p$ . Thus it is easier for a Cerenkov to separate kaons from protons than pions from kaons.

The transition-radiation detector (TRD) is a gamma selector ( $\gamma = E/m \approx p/m$ ) whose gamma resolution,  $\Delta\gamma$ , is defined in terms of the total X-ray energy,  $W$ , detected by the counter\*:

$$\Delta W \approx \frac{\partial W}{\partial \gamma} \cdot \Delta\gamma \approx \text{const.} \Delta\gamma .$$

Kinematically, this is related to the momentum  $p$  of two particles of different masses  $m_0$  and  $m_1$  by:

$$\Delta\gamma \approx p \left( \frac{1}{m_0} - \frac{1}{m_1} \right) .$$

\*See Section 6 for a discussion of the possibility of also measuring  $\gamma$  by the geometric pattern of TR-photons.

Thus it is easier to separate pions from kaons than kaons from protons with TRD; i.e.,  $\Delta\gamma(\pi K) = 5.34 \Delta\gamma(Kp)$  for the same  $p$ .

Thus the gas Cerenkov counter and the Transition Radiation Detector should be regarded as complementary tools in particle identification in a high-momentum beam. As shown in Figure 4, the TRD pion signal is  $\sim 15 \times$  the kaon signal at 400 GeV/c, whereas the gas Cerenkov is pressed to discriminate pions from kaons (but can more readily distinguish both mesons from protons). The obvious solution is to demand a TRD Cerenkov coincidence for pions, while putting the TRD in anti-coincidence for kaons.

Comparison of Particle Identification Between TRD and Gas Cerenkov in Bubble-Chamber Beamline. It is proposed that the Phase I TRD's output be compared with the output of the 40-meter threshold-differential gas Cerenkov<sup>(10)</sup> already installed in the bubble-chamber beamline. Particle-by-particle comparison over a range of momenta should define the useful range for each device, as well as the range of "complementarity."

The low-intensity beam in the bubble-chamber beam is ideal for the comparative tests proposed here.

The design report on the existing gas Cerenkov<sup>(10)</sup> states a small Cerenkov angle ( $\theta = 2.5$  mr) for kaons and an expected resolution  $\Delta\theta = \pm 0.16$  mr., dominated by beam divergence. This implies  $\Delta\beta \approx 0.8 \times 10^{-6}$ , or a limiting  $\pi$ -K separation

momentum of 370 GeV/c. For the 40-meter section of Cerenkov constructed (the final design is 80 meters, in two sections), the expected yield of photoelectrons is approximately,<sup>(1)</sup>

$$N = \epsilon A L \theta^2 = 2.0 \text{ photoelectrons,}$$

where  $\epsilon$  = light collection efficiency,  $L = 4000$  cm, and  $A = 100$  (depends upon phototube response). This average photoelectron yield would predict an efficiency of about 87%.

The Phase I TRD proposed here is expected to operate with an average of 5.2 photoelectrons in the xenon proportional chamber. The pulse-height distribution (Figure 5) suggests that 400 GeV/c pions can be detected with 96% efficiency, while rejecting 96% of the kaons (and all of the protons). The TRD is not sensitive to beam divergence.

Improvements in Gas Cerenkov Counters and Transition Radiation Detectors. The gas Cerenkov technique is very well developed into a precision tool for velocity measurement. The "state of the art" includes the DISC-type Cerenkov<sup>(1)</sup> which provides the ultimate in resolution. The DISC counter being built for NAL<sup>(11)</sup> utilizes 10 meters of helium at 30 atmospheres (about 5.4 gm/cm<sup>2</sup> of helium); this could conceivably be used in the bubble-chamber beam. Meunier, et al. claim limiting momenta for  $\pi$ -K separation above 500 GeV/c<sup>(1)</sup>.

The TRD is still "to be proved": the technique is in its infancy. Hopefully these tests, built upon previous work by ourselves and others, will demonstrate the present utility and future directions for development.

## V. DETAILS OF THE PHASE I NAL TR-DETECTOR

A few of the more important details of the Phase I TR-detector are covered in this section.

Beryllium Foil Radiator. The reaction of many to the proposed use of Beryllium foils is "...but isn't beryllium expensive?" The answer is, "Yes, but it's worth it!" The reduced X-ray absorption in Be, which makes possible a single radiator of 1000 foils, simplifies the design. The actual expense for materials is about \$3500 for .001" Be foils (250 4" x 5" x .001" sheets at \$14.00, each sheet being cut into four 2" x 2½" foils). Cutting of Be is non-trivial, but is done routinely at the Lawrence Radiation Laboratory.

The bubble-chamber beam must be kept reasonably free of contamination by secondary particles, at least when it reaches the bubble chamber. It is estimated<sup>(12)</sup> that "up to 10 gm/cm<sup>2</sup>" of material in the beam might be tolerable, if followed by a sweeping magnet and if located well upstream of the bubble chamber. The 1000 .001" Be foils constitute 4.7 gm/cm<sup>2</sup> (0.095 collision lengths). We propose to locate the radiator just upstream of the horizontal bending magnets in Enclosure 112, which is followed by vertical bending magnets, a drift space, more bending in Enclosure 114, and a long distance to the bubble chamber.

Secondary Electrons Produced by Kaons in Be Foils. It is possible (in principle) for "knock-on" electrons produced by atomic collisions of kaons or protons in the radiator to

produce TR in the radiator.....or synchrotron radiation in the bending magnet and thus simulate pions. The maximum energy of the knock-ons is essentially the incident momentum of the kaon or proton. Thus there exists a continuous spectrum of ultrarelativistic electrons. This spectrum is peaked at low energies, however, and the number of knock-on electrons per heavy particle is quite low. Using the standard treatment<sup>(13)</sup> for collision processes involving electrons, we have calculated the probability that a 400 GeV/c K should produce a knock-on electron with momentum above 400 MeV/c (the same  $\gamma$  as the kaon) in 4.7 gm/cm<sup>2</sup> of Be. This probability is only  $8 \times 10^{-4}$ .

This same low yield enables us to dismiss worries about magnetic bremsstrahlung ("synchrotron radiation") in the bending magnets following the radiator. Although electrons momenta lower than 400 MeV/c will also radiate, such electrons will be deflected away from the detector direction in such short distances that this background is also negligible.

Xenon MWPC Detector. Our experience with argon, krypton, and xenon MWPC detectors has shown that the detector should be "thick" to TR-X-rays and "thin" to background photons and charged particles. Figure 8 clearly shows that our 1.5 cm chambers are "too thin" for TR-photons above about 10 KeV. In our SLAC MS runs, we "stacked" eight MWPC together to give 12 cm of xenon gas, but the individual chamber windows (and intervening air between chambers) still absorbed much

of the fluorescent escape photon energy and the long range recoil electron energy. About 50% of the energy deposited by TR-X-rays in 12 cm xenon gas was lost in the SLAC setup. We propose, therefore, to build a new multi-compartment chamber with 20 cm of xenon. One design involves ten 2-cm MWPC compartments, separated by thin electrical cathode planes, within a common gas barrier. Fluorescent escape photons have a good probability of being absorbed in 20 cm of xenon. The high energy ( $> 25$  KeV) photoelectrons and Auger electrons, which previously escaped from 1.5 cm MWPCs, will ionize the xenon of adjacent compartments. In this manner, we anticipate absorbing most of the 50% "lost" in the SLAC runs.

The predicted yields in Figure 4 and 5 were calculated for a thinner (10 cm xenon) chamber, so these are slightly conservative estimates.

As indicated earlier, the value of having 10 separate "cells" within the detector to sample the ionization-vs-depth is that this gives the "signature" of TR and helps eliminate background. At the same time, the "sum signal" gives the total deposited X-ray energy. (As noted in Section VI, the separate cells, equipped with positional readout, can also detect the spatial distribution of individual TR-photons.)

Data-Handling System; On-Line Computer. We propose to use the Hawaii-developed CAMAC-NOVA data-handling system, already used in the SLAC TR-run of August 1972. The basic elements of the system are:

- (1) Two ADC 8-channel units (LeCroy Model 2248).
- (2) CAMAC databus system, with crate controller.
- (3) NOVA-800 computer system, with disk file and mag-tape CRT display (Tektronix 611) and Teletypewriter.

This forms a versatile data-acquisition system which can handle (store and readout) 16 channels of 256-bit analogue signals (pulse heights). The digitizing time of the LeCroy 2248 is 150 microseconds, so that low intensity beams (i.e., bubble-chamber beams) are necessary. (Faster digitizers are available.)

In our SLAC runs we found it useful to digitize the output of the Shower Counter. At NAL it may be desirable to store the fast-counter information also.

Tagging for the 30-Inch Bubble Chamber. The synchronization of the TR-signals with those of the gas Cerenkov is most important for Phase I. We see no inherent difficulty in doing this, despite the considerable distance between detectors. Presumably, the method used will be similar to the synchronization between the MIT- et al. "tagging" wire chambers and the Cerenkov.

The details of each event would be recorded on tape for TR, and compared with the Cerenkov "decision" and/or the bubble-chamber event.

## VI. COHERENT TRANSITION RADIATION; PHASE II TR-DETECTOR

The Phase I TR-detector was chosen as the simplest possible arrangement which promised practical pion-vs.-kaon particle identification. No attempt to explore further the "physics" of Transition Radiation was proposed. Instead, we sought to optimize proven methods of TR-generation and detection.

In Phase II, we hope to detect coherent transition radiation not only for its physics interest but also to develop a more precise TR-detector. An NAL investigation looks promising because:

- (1) NAL pions offer the first practical opportunity to detect coherent TR, since focused beams of "heavy" particles of high  $\gamma$  are needed. (Multiple scattering of electron beams "wash out" coherent effects.);
- (2) A modest extension of our Phase I apparatus, using MWPC delay-line readout of position and charge, seems adequate for recording coherent TR effects;
- (3) In principle, coherent TR offers increased precision in measuring  $\gamma = E/m$ , and thus better mass resolution, for the same total TR-signal;
- (4) Further development of TR-detectors could lead to large solid angle arrays; e.g., identification of secondary particles behind bubble chambers, etc. (Unlike gas Cerenkovs, the TR-detectors do not require collimation.)

Since the future plans of NAL include the possibility of going to 1000 GeV, where the TR-effects will be even greater than at 400-500 GeV, it seems reasonable to pursue the TR-detector development beyond its most elementary applications.

Angular Distribution of Coherent TR. In Section III, we listed the basic differential-energy distribution (Equation (7)) that included the "diffraction-grating term,"

$$f_N = \left( \frac{\sin \frac{N\phi}{2}}{\sin \frac{\phi}{2}} \right)^2, \quad (12)$$

which applies for no absorption in the foils. The phase shift per foil-gap module,  $\phi = a_f + a_g$ , where  $a_f$  and  $a_g$  are linear thicknesses of foil and gap measured in units of "formation zones"  $Z_f$  and  $Z_g$ , is the important variable. Clearly, for very small  $\phi$ ,  $f_N \simeq N^2$ , but such small phases are of little importance since the single-foil yield decreases rapidly as thicknesses go below  $Z$ . Singularities of  $f_N$  exist for all values of  $(\phi/2) = m\pi$  so that many "peaks" in the angular distribution are expected.

Figure 12 shows a plot of  $f_N$  as a function of angle for two different TR-X-ray energies (10 KeV and 5 KeV). The angle,  $\theta$ , is related to the phase  $\phi$  quadratically:

$$\phi = \phi_0 + A\theta^2, \quad (13-a)$$

where

$$\phi_0 = \frac{\omega}{2c} \left[ (\gamma^{-2} + \epsilon_f^2) t_f + (\gamma^{-2} + \epsilon_g^2) t_g \right] \quad (13-b)$$

and

$$A = \frac{\omega}{2c} (t_f + t_g) . \quad (13-c)$$

Thus the value of the k-th "peak" value of angle,  $\theta_k$ , is given by

$$\theta_k = \sqrt{\frac{2k\pi - \phi_0}{A}} . \quad (14)$$

Note that these peaks change with X-ray energy as well as  $\gamma$ .

Self-absorption in the foils and gap (if not vacuum) attenuate the amplitudes generated by each surface. The factor,  $f_N$ , is modified accordingly:

$$f_N = e^{-(N-1)b} \left\{ \frac{\cosh Nb - \cos N\phi}{\cosh b - \cos \phi} \right\}, \quad (15)$$

where  $b = b_f + b_g$  is the absorption "angle" in the foil-gap such that  $b_f = \frac{1}{2}(\mu\rho t)_{\text{foil}}$  and  $b_g = \frac{1}{2}(\mu\rho t)_{\text{gap}}$  for the particular X-ray energy involved. As expected, absorption decreases and broadens the peaks and tends to suppress the oscillations between major peaks. Note that the peak angles,  $\theta_k$ , are unchanged by absorption; the condition is still  $\phi = 2m\pi$  for principal peaks, and there are N secondary oscillations between principal peaks.

Figure 12 includes the effects of X-ray absorption in Mylar. Note that the secondary oscillations are strongly suppressed by the large absorption at lower X-ray energies (5 KeV curve). However, it can be shown that all of the peaks in  $f_N$  have equal amplitudes and widths when plotted vs.  $\phi = \phi_0 + A\theta^2$ . The peaks are equally spaced ( $\Delta\phi = 2\pi$ ) on such a "universal plot." This greatly simplifies calcu-

lation of the integration of the differential TR-yield over solid angle. The total yield does not increase without limit, since

$$\frac{d^2W}{d\theta^2} = f_0 \cdot f_1 \cdot f_N, \quad (16)$$

where  $f_0$  is the single-surface yield

$$f_0 = \frac{\alpha}{8\pi} \theta^3 \left(\frac{\omega_f}{c}\right)^4 Z_f^2 Z_g^2, \quad (17)$$

and the single-foil factor ( $\sin^2 \frac{1}{2}a_f$ , without absorption) is:

$$f_1 = 4e^{-b_f} \left[ \cosh b_f - \cos a_f \right], \quad (18)$$

and the product of  $f_0 \cdot f_1$  gradually decreases with angle since  $Z_f^2 Z_g^2 \sim \theta^{-4}$  for large  $\theta$ .

In any event,  $f_N$  is strongly angle dependent for a given X-ray energy. If the X-ray energy  $E$  is measured with an accuracy  $\Delta E$ , then the angular cone  $\theta(E)$  will have fractional width

$$\frac{\Delta\theta}{\theta} = 0.42 \left(\frac{\Delta E}{E}\right),$$

for  $E = 10$  KeV,  $\gamma = 2860$ , and peak  $\theta_2 = 0.540$  mrad. For the same conditions, the angular spread due to variation in  $\gamma$  is:

$$\frac{\Delta\theta}{\theta} = 0.41 \left(\frac{\Delta\gamma}{\gamma}\right).$$

Thus if  $\Delta E/E = 0.21$  (FWHM), then the pion cone width  $\Delta\theta/\theta$  would also be about ~~20~~<sup>8</sup>%. The resolution in  $\gamma$  would also be about 20%. The energy resolution is our present measured value. The resolution in  $\gamma$  is 10x better than required to distinguish pions from kaons.

Multiple Scattering in the Foils. The multiple scattering angle (rms., space) of an ultrarelativistic particle of momentum  $p$  in traversing  $X$  radiation lengths is given by the familiar formula,

$$\alpha = \frac{E_s}{p} \sqrt{X}, \quad (19)$$

where  $E_s = 21$  MeV. The particle's mass does not enter.

A typical "peak angle" for TR emitted by a particle of momentum  $p \approx \gamma M$  is:

$$\theta_1 \approx 1/\gamma \approx M/p.$$

Thus the ratio of TR-angle to rms-scattering angle is passing through one foil is:

$$\theta_1/\alpha \approx M/E_s \sqrt{X}. \quad (20)$$

Note that this ratio is independent of momentum but depends upon particle mass.

Our SLAC runs used electrons and .002" polyethylene foils: the scattering angle was 4.0 times the TR-angle  $\theta_1$ . Thus no coherent effects could be expected.

At NAL with pions and kaons passing through .001" Be foils, the ratio of scattering/TR-angles is 1:25 (pions) and 1:89 (kaons) for one foil. The total scattering angle increases as  $\sqrt{X}$  so that scattering begins to "fuzz" the angular peaks after 1000 foils. A detailed quantitative calculation is planned. However, it is clear that coherent effects should be quite visible.

Energy and Position Detection with Delay-Line Readout of MWPC. Our SLAC TR multi-wire proportional chambers were

originally built for the "proportional quantameter"<sup>(14)</sup> (i.e., a photon shower counter consisting of MWPC sandwiched between lead sheets). We were successful in adapting the electromagnetic delay-line readout idea of Perez-Mendez<sup>(15)</sup> to our chambers, reading out both position and charge (ionization current to center wires or induced on cathode wires). The accuracy in position was  $\frac{1}{2}$ -wire spacing; the linearity of charge readout was good to about 2%.

The EMI development (Hawaii-LBL/Stevenson collaboration) utilizes MWPC delay-line readout of position, with measured accuracy of about 2 mm (5-mm wire spacing). The electronics system is fully developed for reading out 30 chambers simultaneously.

Thus we see no great difficulty with the concept of reading out pulse height and position of 5 to 10 X-ray photons detected in about 8 chamber compartments in a xenon MWPC detector. The angular resolution required ( $\pm 0.1$  mrad) corresponds to  $\pm 5$  mm at the detector. Only 1 or 2 photons maximum per delay line would be read out in one pulse, so two-pulse resolution is not critical.

Thus, with extension of the Phase I setup by adding delay lines and associated readout electronics, it would be possible to study coherent TR and seek to develop an improved resolution in  $\gamma$ .

## VII. SCHEDULE, PERSONNEL, AND BUDGET

Although this proposal must be judged primarily on its intrinsic value to NAL's present and future experimental programs, it may be appropriate to indicate briefly our concept of the time schedule, personnel, and budget involved. These three topics are obviously inextricably intertwined, but at least we can visualize a "scenario."

Time Schedule. Phase I is closely tied to intercomparison with the gas Cerenkov now operating in the 30" BC beamline. The Phase I instrumentation is relatively simple, assuming that the Hawaii CAMAC-NOVA system is available (it is scheduled to be released from EMI operation ~ June 1973, when NAL will provide a PDP-11). The principal problems are (a) to construct the Be radiator, (b) build a multi-cell xenon MWPC, and (c) establish suitable electronics facilities near Enclosure 114. If the personnel and budget listed below are available soon, it should be possible to begin Cerenkov-TR comparisons near the end of 1973.

Phase II would not be undertaken unless Phase I is successful. However, plans for Phase II should be made now since this will affect the design of Phase I chambers (provision for adding delay-line readout). The additional expense of delay lines and associated electronics would be deferred until Phase I is complete. The time scale of Phase I is somewhat difficult to estimate, but it seems possible to obtain useful results during calendar year 1974.

Personnel. The previous TR-experiments performed by the Hawaii-Maryland-Oxford collaboration involved very little beam-on time: 48 hours (Bevatron) and 100 hours (SLAC). The "run-team" was together each time for only about one month. The instrumentation beforehand did involve several man-months for the SLAC run. However, only one physicist (Mr. Tomotaro Katsura) has been on the project full-time continuously. The bulk of the effort has been done by "part-time" efforts by faculty members and postdocs who were deeply involved in other, higher priority projects (such as the EMI for Hawaii, and the New Mexico cosmic-ray project for Maryland personnel).

We will be able to involve most (but not all) of the previous Hawaii-Maryland-Oxford team in this NAL project on much the same basis. For example, the UH-LBL-NAL EMI project involves Dr. Fred Harris (now in residence at NAL) and Dr. Sherwood Parker (commuting regularly between LBL and NAL) who are key "Transition Radiators." Hawaii faculty members involved in both EMI and TR are Dr. Victor Stenger and Dr. Vince Peterson; Maryland counterparts are Dr. Robert Ellsworth and Dr. Gaurang B. Yodh. Mr. Tomotaro Katsura may be available during summer 1973 and perhaps longer. Thus we have much experience on hand (part-time) to move the TR-development forward.

At the same time, we recognize that the stakes are much higher at NAL, and the problems may turn out to be considerably more difficult than at Berkeley or SLAC. If the comparison

between TR-detector and Cerenkov is to be made properly, both detectors must be operated efficiently at the same time. This will require full-time attention of several physicists. Thus we believe that the following personnel requirements should be established before embarking upon this development:

- (a) Two physicists working full-time at NAL on the Cerenkov-TR comparison. We have in mind postdocs from the universities (one each).
- (b) A part-time NAL collaborator, preferably someone intimately associated with the Cerenkov counter operation.
- (c) University group backup on design and development of better X-ray detectors, analysis of running data, etc.

Technical personnel will be needed from time-to-time, both at NAL and at home, for instrumentation jobs. However, these needs are much smaller than the physicist requirements, both in time and in budget.

Budget. The following very brief outline of the proposed "division of responsibilities" in budgetary matters between the universities and NAL may be useful.

<u>Personnel:</u> (in FTE)	<u>UH</u>	<u>MD</u>	<u>NAL</u>
2 postdocs	1.0	1.0	--
NAL staff	--	--	0.25
Faculty (part-time)	0.25	0.25	--
Other Ph.D. staff	0.25	0.25	--

Technicians . . . . .	0.25	0.25	0.50
Students . . . . .	<u>?</u>	<u>?</u>	<u>?</u>
Total . . . . .	1.75	1.75	0.75

Equipment & Construction:

Foil radiators (Be). . . . .	X	X	--
X-ray detectors (MWPC) . . . . .	X	X	--
Data-acquisition system . . . . .	X	--	--
Fast electronics . . . . .	--	X	--
Vacuum system (16" pipe) . . . . .	--	--	X

Operations:

Accelerator signals. . . . .	--	--	X
Coordination with Cerenkov signal . . . . .	--	--	X
Computer analysis . . . . .	X	X	--
Portakamp for electronics. . . . .	--	--	X
Travel . . . . .	X	X	--

As a rough estimate of total costs, over a two-year period, for both Phase I and Phase II, we estimate:

Personnel: (4.25 FTE, with OH) . . . . . \$170 K

Equipment:

Already available for use . . . . .	50 K
New purchase . . . . .	10 K
Construction (except Portakamp). . . . .	20 K

Operations: (including computer time)

\$2 K per month for 2 years . . . . .	48 K
---------------------------------------	------

## REFERENCES

1. M. Benot, J. Litt, and R. Meunier, "Cerenkov Counters for Particle Identification at High Energies," CERN Report, (July 1972).
2. V. L. Ginzburg and I. M. Frank, JETP 16, 15 (1946).
3. (a) A. I. Alikhanian, G. M. Garibian, K. A. Ispirian, A. G. Oganessian, Proc. Intern. Conf. on High Energy Instr., Versailles (1968); (b) A. I. Alikhanian, G. M. Garibian, K. A. Ispirian, A. G. Oganessian, Yerevan Phys. Inst. Report (1969); (c) A. I. Alikhanian, K. A. Ispirian, A. G. Oganessian, A. G. Tamanian, Nucl. Instr. and Meth. 89, 147 (1970).
4. G. M. Garibian, "Theoretical Foundations of Transition Radiation," Yerevan report EφN-Tφ-13 (1970), (summary and references to earlier work).
5. (a) J. Oostens, S. Prunster, C. L. Wang, and Luke C. L. Yuan, Phys. Rev. Letters 19, 541 (1967); (b) S. Prunster, C. L. Wang, L.C.L. Yuan, and J. Oostens, Phys. Letters 28B, 47 (1968).
6. (a) Luke C. L. Yuan, C. L. Yang, and S. Prunster, Phys. Rev. Letters 23, 496 (1969); (b) Luke C. L. Yuan, C. L. Wang, H. Uto, and S. Prunster, Phys. Letters 31B, 603 (1970); (c) Luke C. L. Yuan, C. L. Wang, H. Uto, and S. Prunster, Phys. Rev. Letters 25, 1513 (1970); (d) H. Uto, Luke C. L. Yuan, G. F. Dell, and C. L. Wang, Nucl. Instr. and Meth. 97, 389 (1971).

7. F. Harris, T. Katsura, S. I. Parker, V. Z. Peterson, R. W. Ellsworth, G. B. Yodh, W.W.M. Allison, C. B. Brooks, J. H. Cobb, and J. H. Mulvey, "The Experimental Identification of Individual Particles by the Observation of Transition Radiation in the X-Ray Region," Nucl. Instr. and Meth. (in press).
8. SLAC experiment (August 1972) by Hawaii-Maryland-Oxford collaboration (Report in preparation).
9. J. E. Bateman, Nucl. Instr. and Meth. 103, 565 (1972).
10. J. Lach and S. Pruss, Appendix A of NAL Report TM-298.
11. G. Cocconi, J. Litt, and R. Meunier, "A High-Resolution Disc Cerenkov Counter for NAL," NAL Report TM-351 (1971).
12. L. Voyvodic, private communication.
13. B. Rossi, "High-Energy Particles" (Prentice Hall, 1952), Chap. 5 (Sec. 5.2).
14. T. Katsura, S. I. Parker, V. Z. Peterson, D. E. Yount and M. L. Stevenson, Nucl. Instr. and Meth. 105, 245 (1972).
15. V. Perez-Mendez, et al., Nucl. Instr. and Meth. 99, 381 (1972).

## Figure Captions

- Fig. 1 The Phase I experimental arrangement shown (a) schematically, and (b) on a scale drawing of the bubble-chamber beamlines. The foil radiator is located in Enclosure 112, the detector in Enclosure 114. Gas Cerenkov, TR-detector, and 30-inch bubble chamber are in the same beamline.
- Fig. 2 The predicted variation of TR-yield with number of 1-mil Be foils in a radiator with 30-mil spacing between foils.  $N$  is the number of photons detected, and  $W$  is the total X-ray TR-energy detected in the xenon detector. Self-absorption limits the maximum useful number of foils. The TR-spectrum used is that generated by 400 GeV/c pions.
- Fig. 3 The predicted single-photon distributions for TR from 400 GeV/c pions and kaons passing through 1000 1-mil Be foils and detected in a 10-cm thick xenon proportional chamber. The K-flux is strongly suppressed by self-absorption due to lower X-ray energies.
- Fig. 4 The total detected TR-yield as a function of charged-particle momentum for pions and kaons. The mean values represent integrals of the detected single-photon distributions.
- Fig. 5 The pulse-height distribution for 400 GeV/c pions and kaons for the detected energy signal in a 10-cm xenon proportional counter. The width of the distribution

includes Poisson statistics of the number of photons as well as the energy distribution of single photons.

Fig. 6 Calculated values of the "formation zone"  $Z(\gamma, E, \theta)$  in air and in polyethylene as a function of X-ray energy.

Fig. 7 Predicted single-photon energy distributions of TR-X-rays produced by 3 GeV/c electrons passing through 100 2-mil polyethylene foils spaced 125 mils apart. The top curve is 200x the yield from a single interface. The "stack" curve includes the interference and absorption effects of 100 foils and represents the energy spectrum emerging from the radiator. The "detected" spectrum is the distribution in energy of single photons detected by eight 1.5 cm xenon MWPC used in the SLAC MS run.

Fig. 8 Calculated energy-detection efficiencies of a 1.5 cm thick gas proportional chamber filled with (a) argon, (b) krypton, or (c) xenon gas at S.T.P., as a function of X-ray energy. The K-absorption edges are apparent. The efficiency is defined as the (ionization energy detected)/(photon energy incident), where the ionizing electrons may come from direct photoelectric effect, absorption of fluorescent photons, or the Auger effect. Fluorescent escape is quite important, particularly in xenon. Range escape is not included in this curve.

Fig. 9 Schematic representation of two different arrays of radiator and detector which have produced useful TR

results. See text for details.

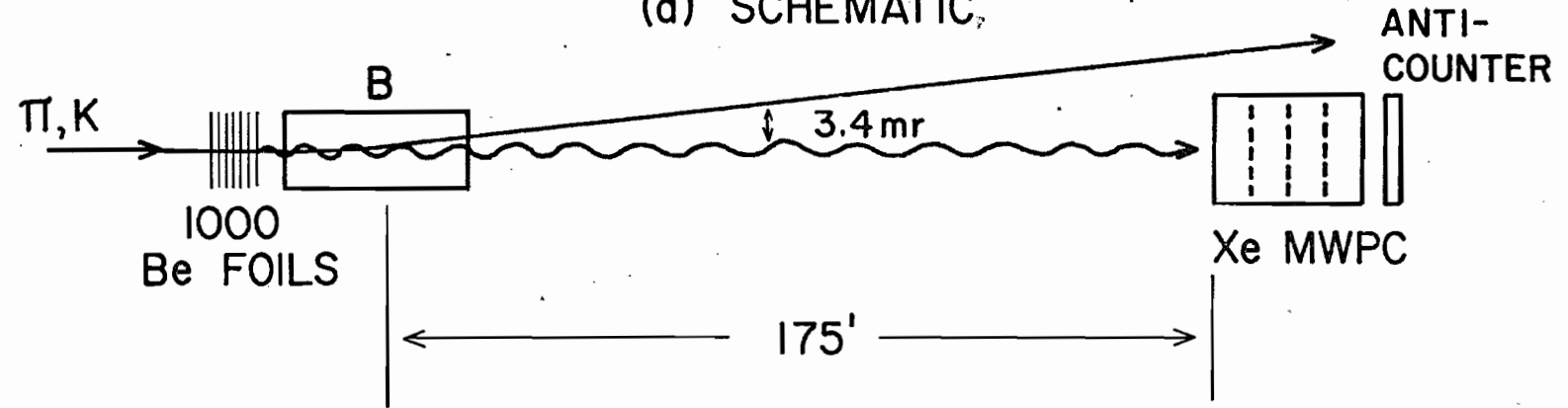
Fig. 10 Preliminary experimental results on total TR-yield from the SLAC "sandwich array" runs with electrons of 3, 9, and 15 GeV/c. The solid curves are predictions based on incoherent TR-production from the sum of eight modules. Each module has a 100-foil Mylar radiator and a 1.5 cm krypton MWPC detector. The detection efficiency used includes not only the krypton curve of Figure 8 but also a factor of 0.62 to account for the "shadowing effect" of chamber wires, absorption in chamber windows, range escape, and the fact that 10% of foils were touching one another.

Fig. 11 Preliminary experimental results from the SLAC "magnetic-separation" array run with 3 GeV/c electrons and eight 1.5-cm xenon MWPC in series. The sum of all 8 pulse heights is shown in (a) for both "radiator" and "equivalent absorber" runs. The distribution of ionization among chambers is shown in (b). Note the attenuation of TR-signal with depth in xenon.

Fig. 12 The theoretically predicted angular variation of the "diffraction-grating" factor,  $f_N(\theta)$ , in the formula for coherent transition radiation. No multiple scattering is assumed, but self-absorption is included.

# PHASE I EXPERIMENTAL ARRANGEMENT

(a) SCHEMATIC



(b) MAGNET LAY-OUT (to scale)

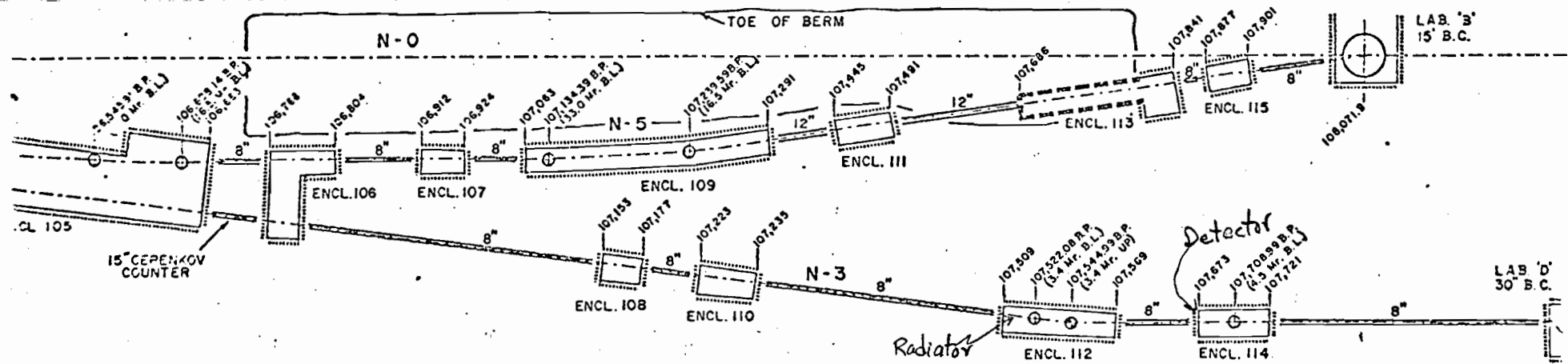


Fig. 1

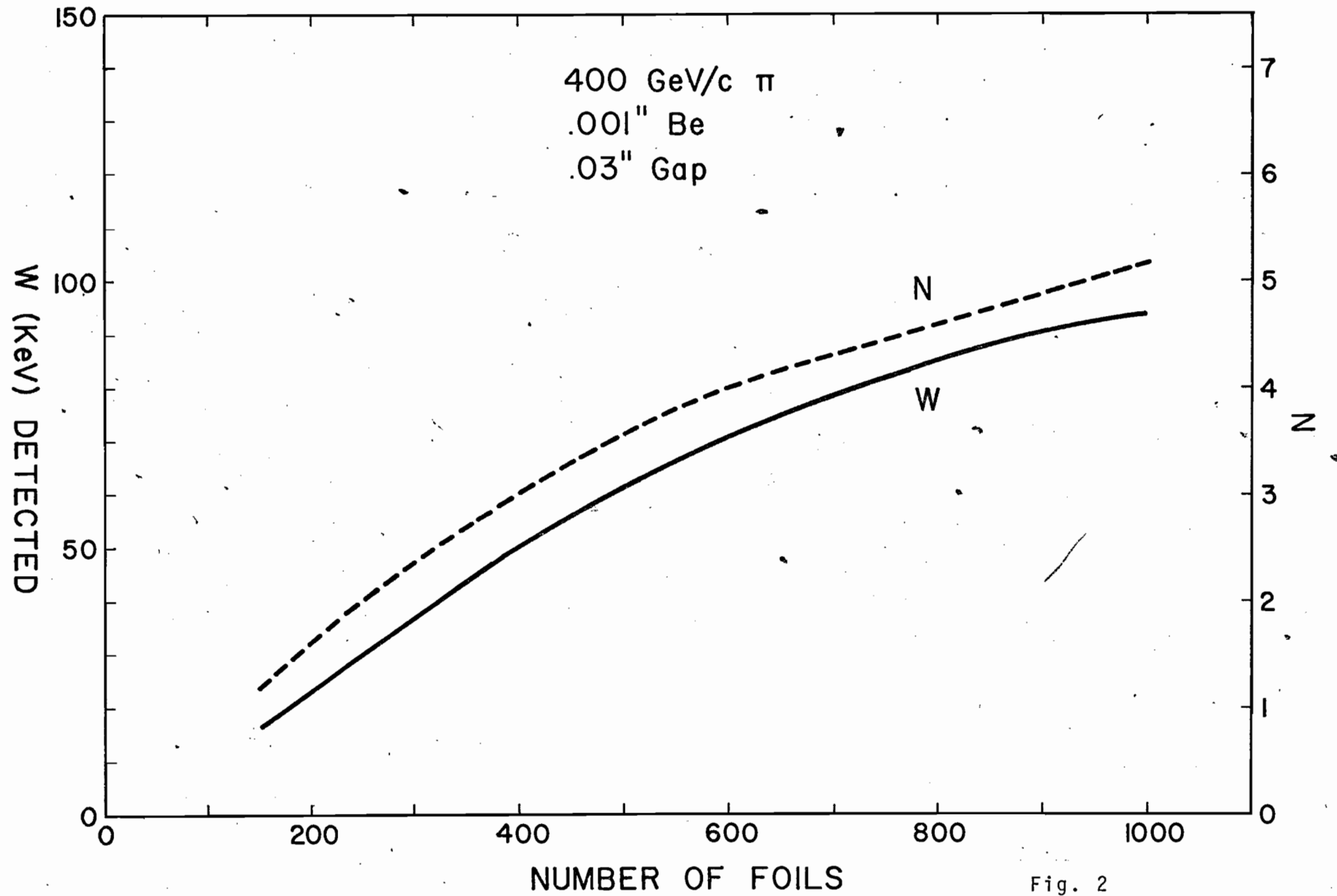


Fig. 2

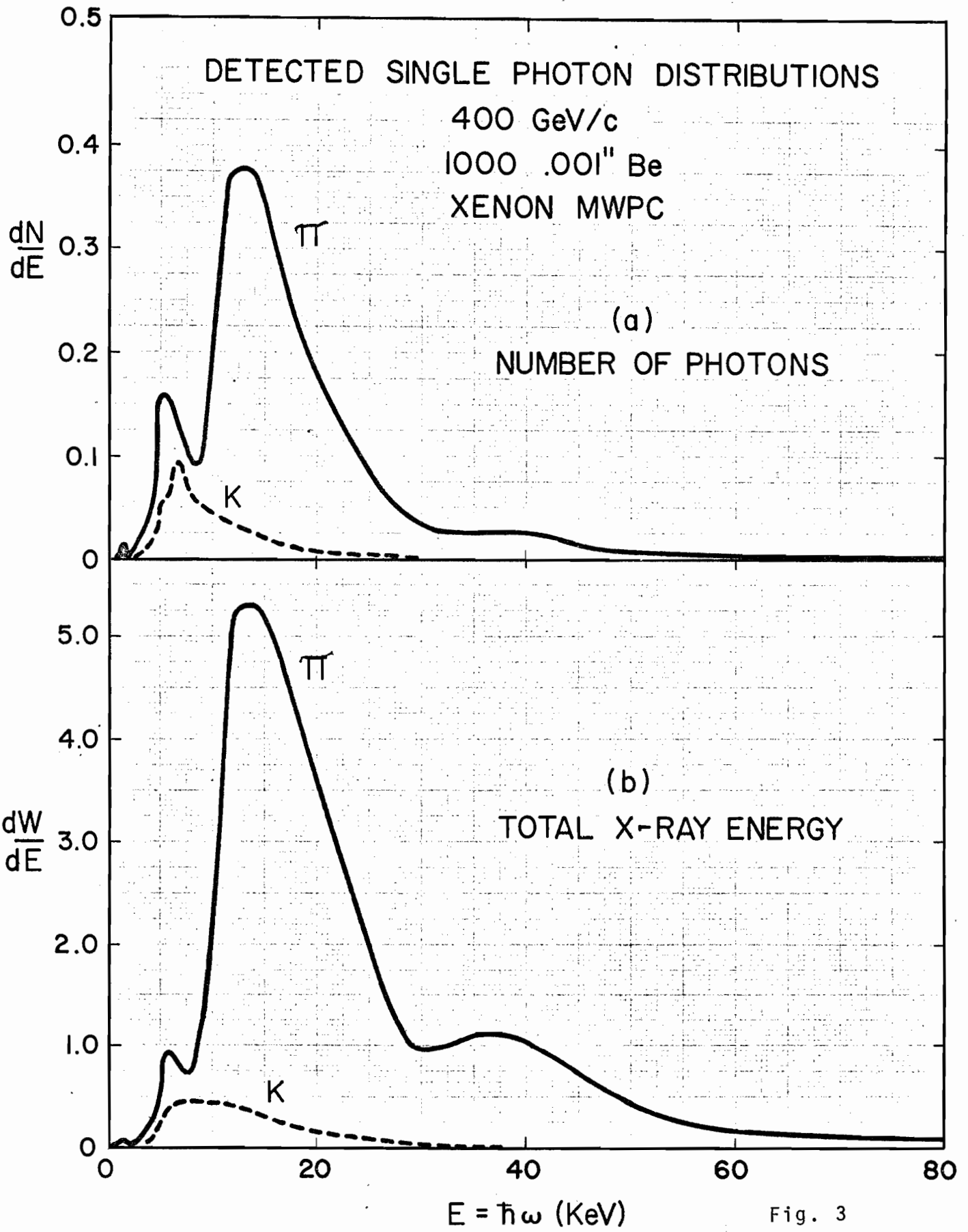
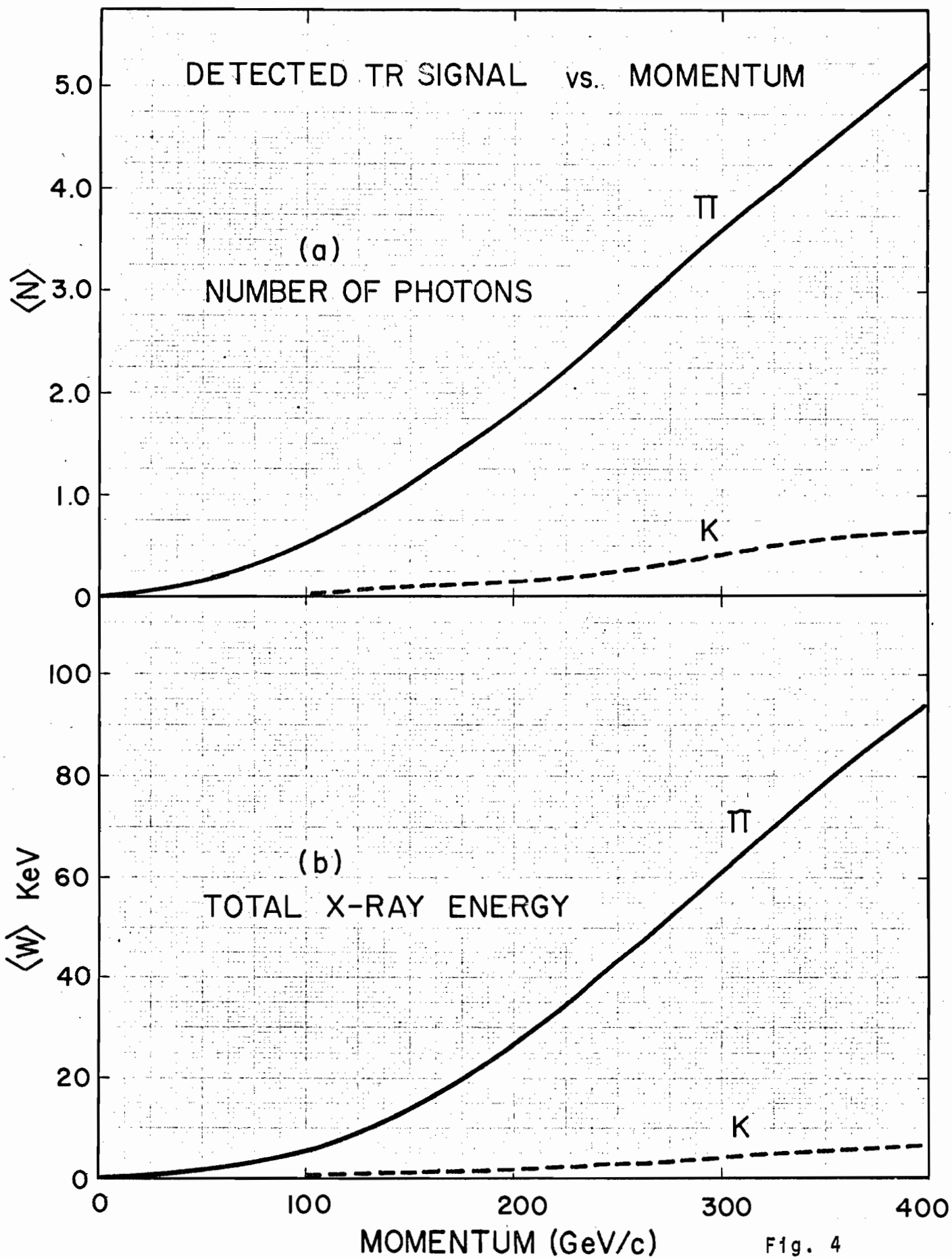
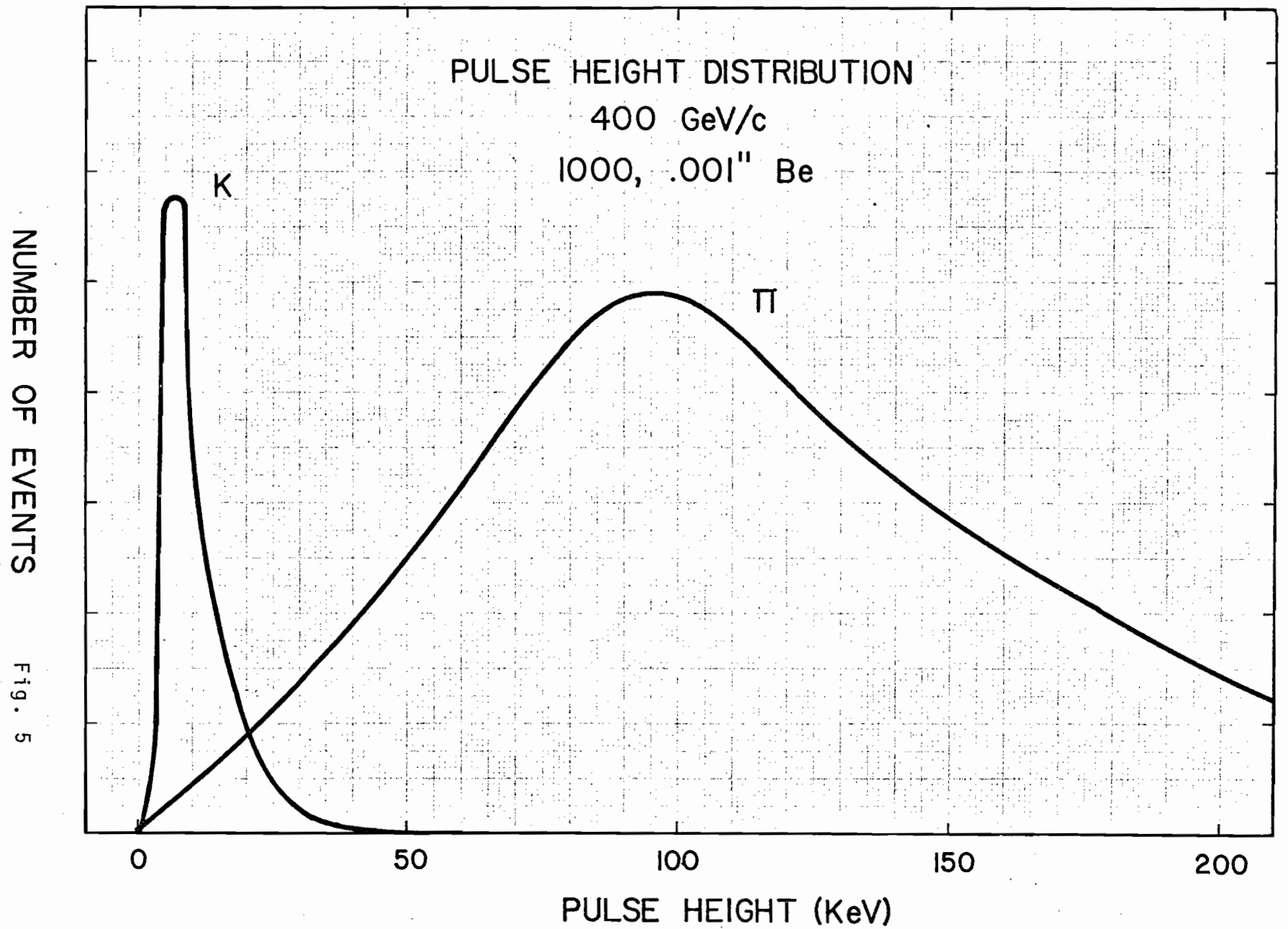


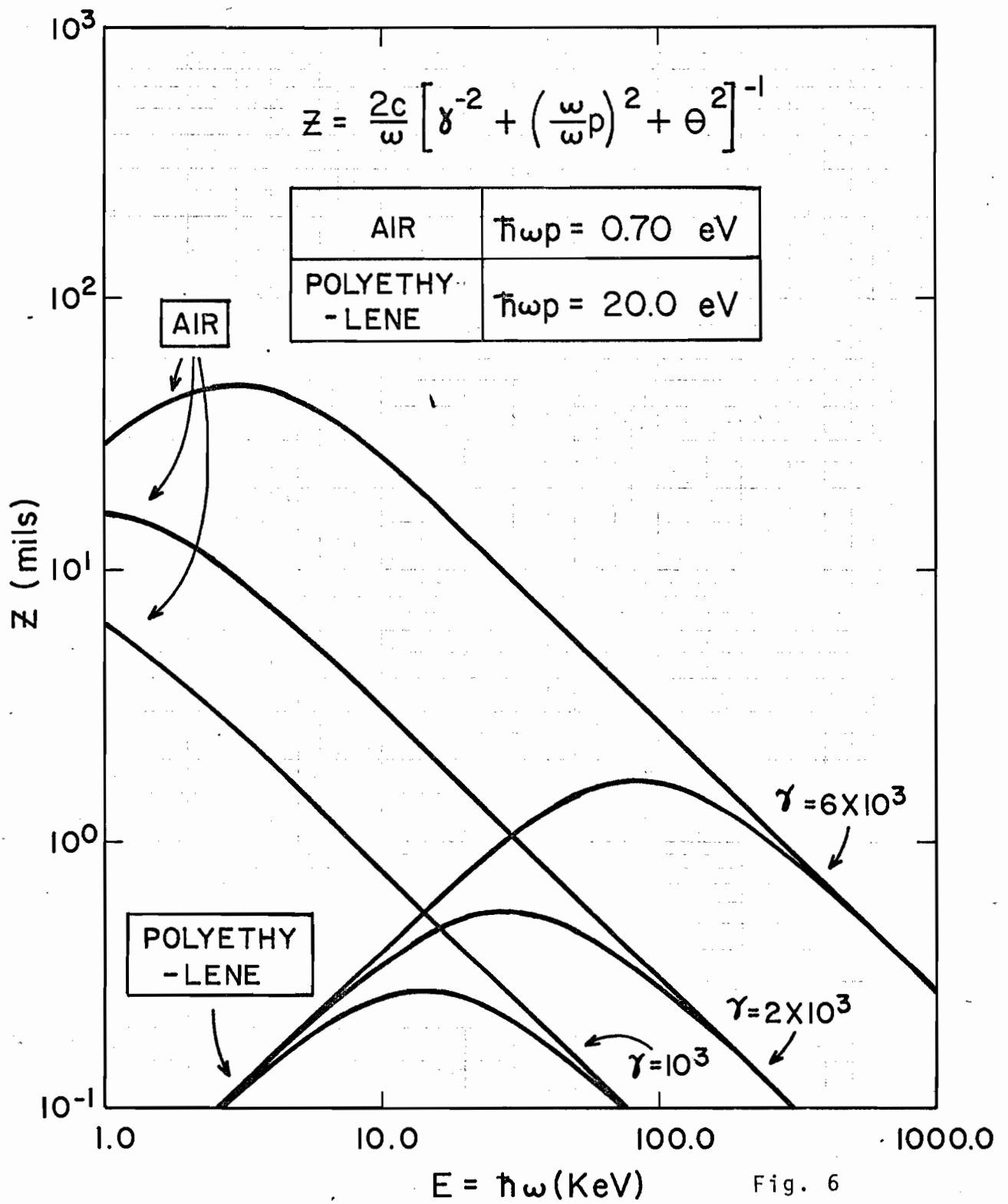
Fig. 3





NUMBER OF EVENTS

Fig. 5



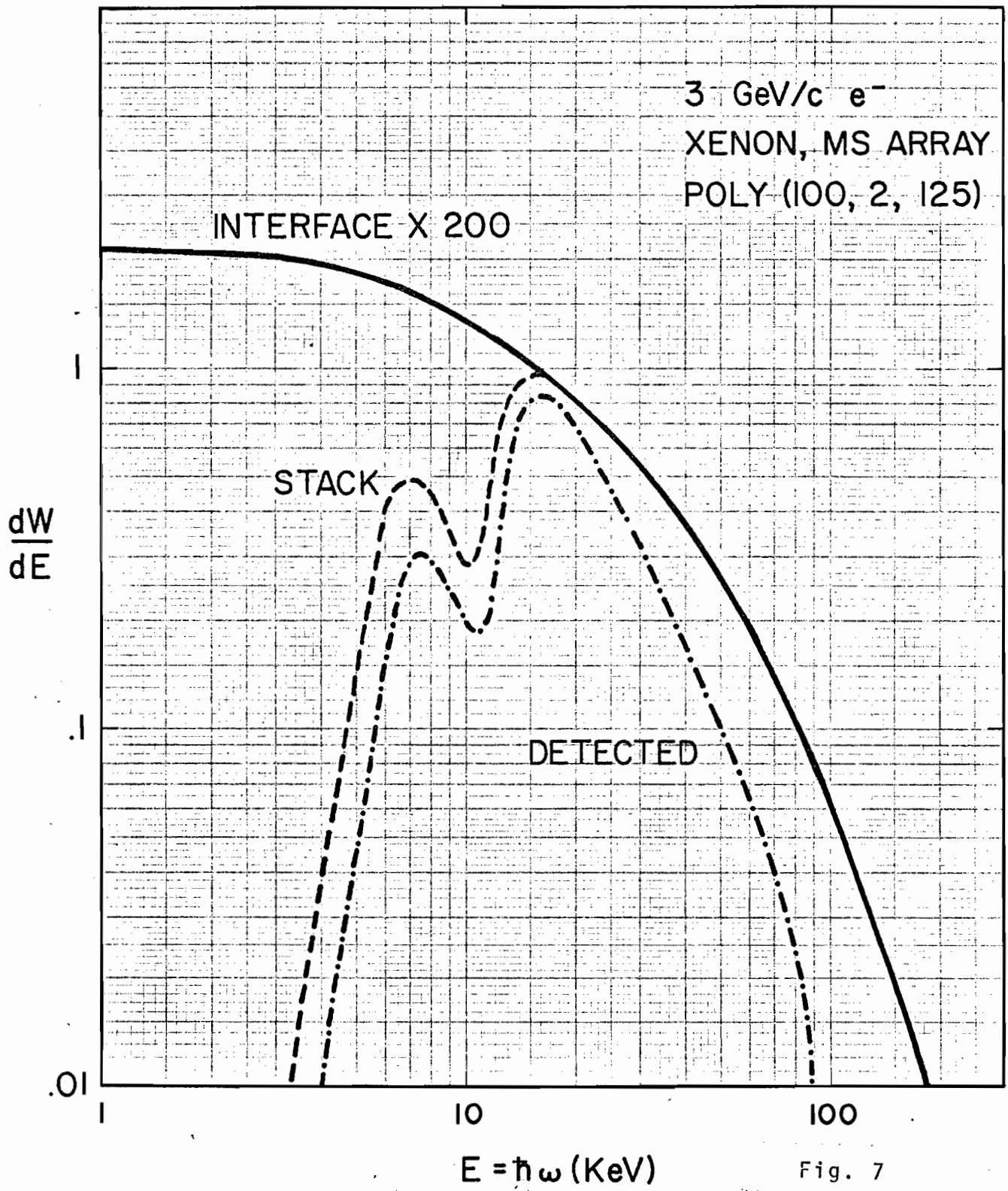


Fig. 7

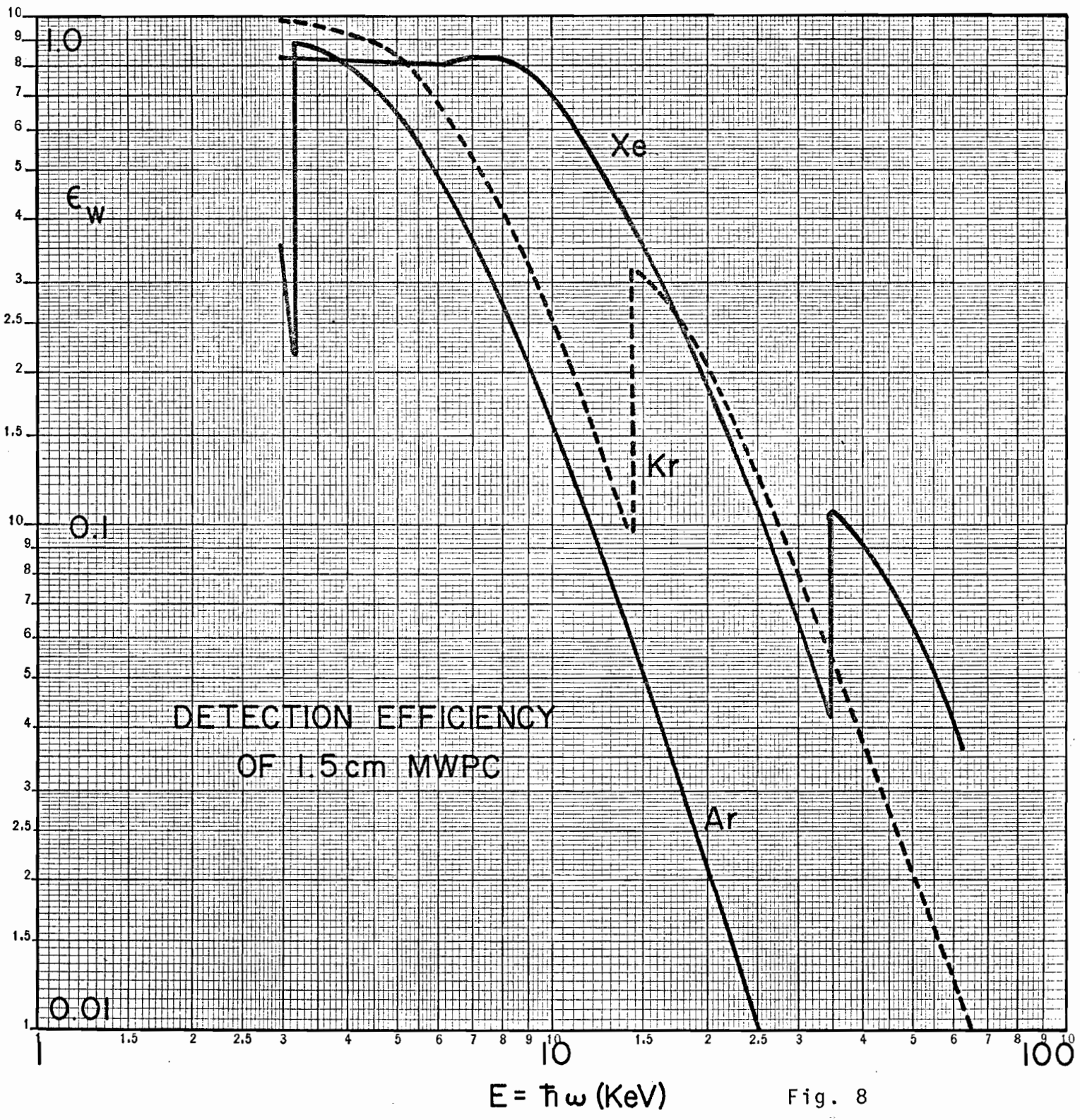
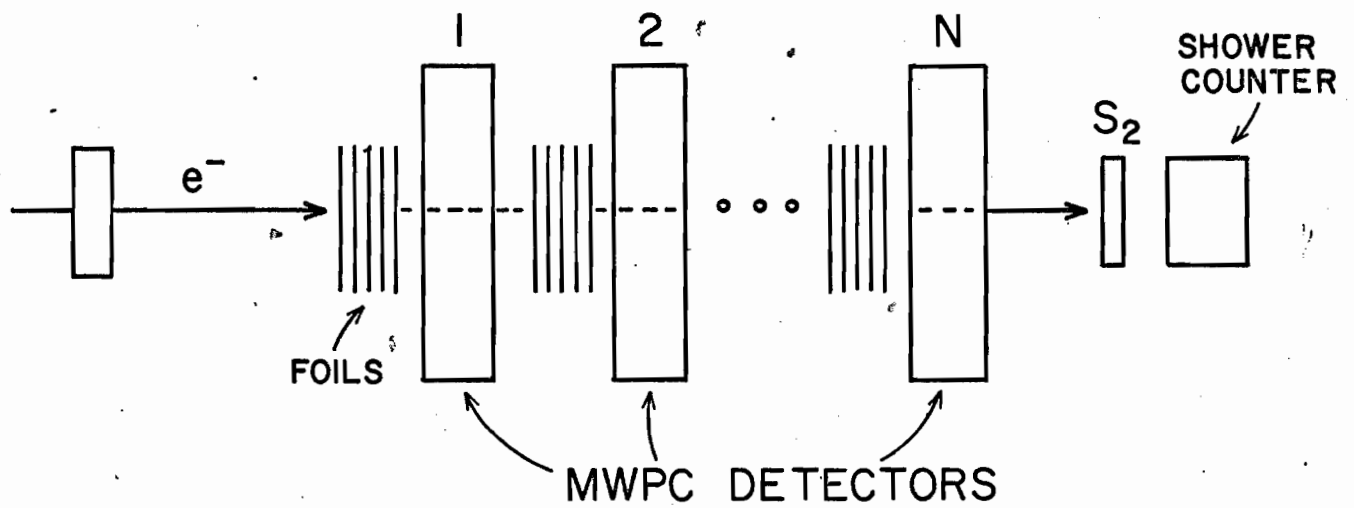


Fig. 8

TR RADIATOR-DETECTOR ARRAYS  
(SCHEMATIC ONLY)

(a) SANDWICH (SW) ARRAY



(b) MAGNETIC SEPARATION (MS) ARRAY

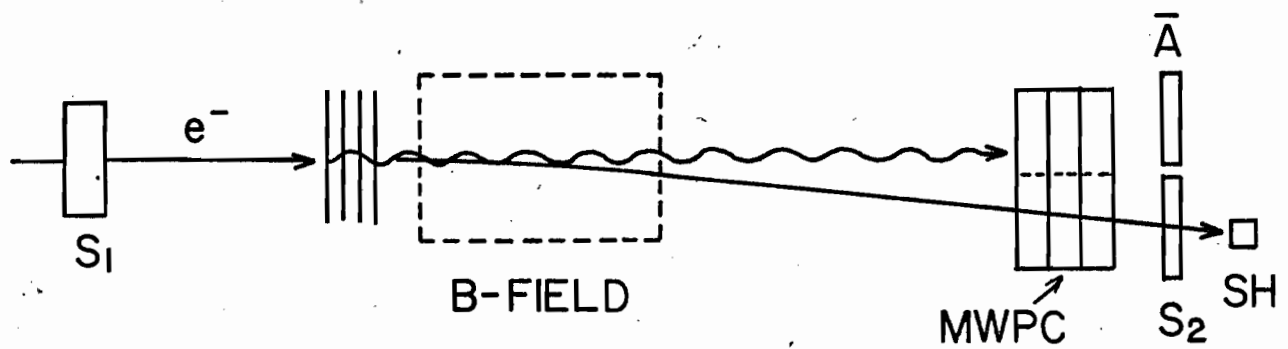


Fig. 9

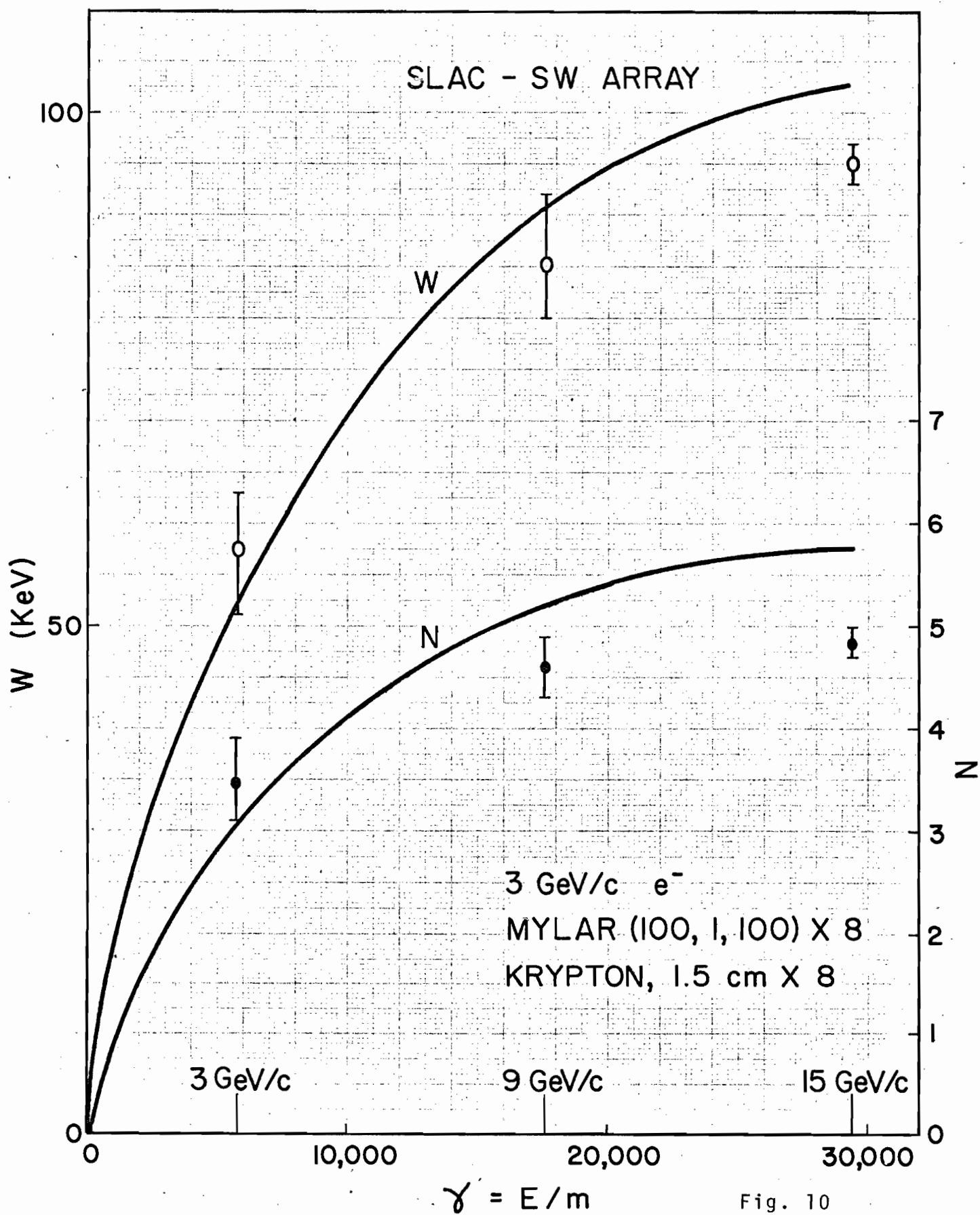


Fig. 10

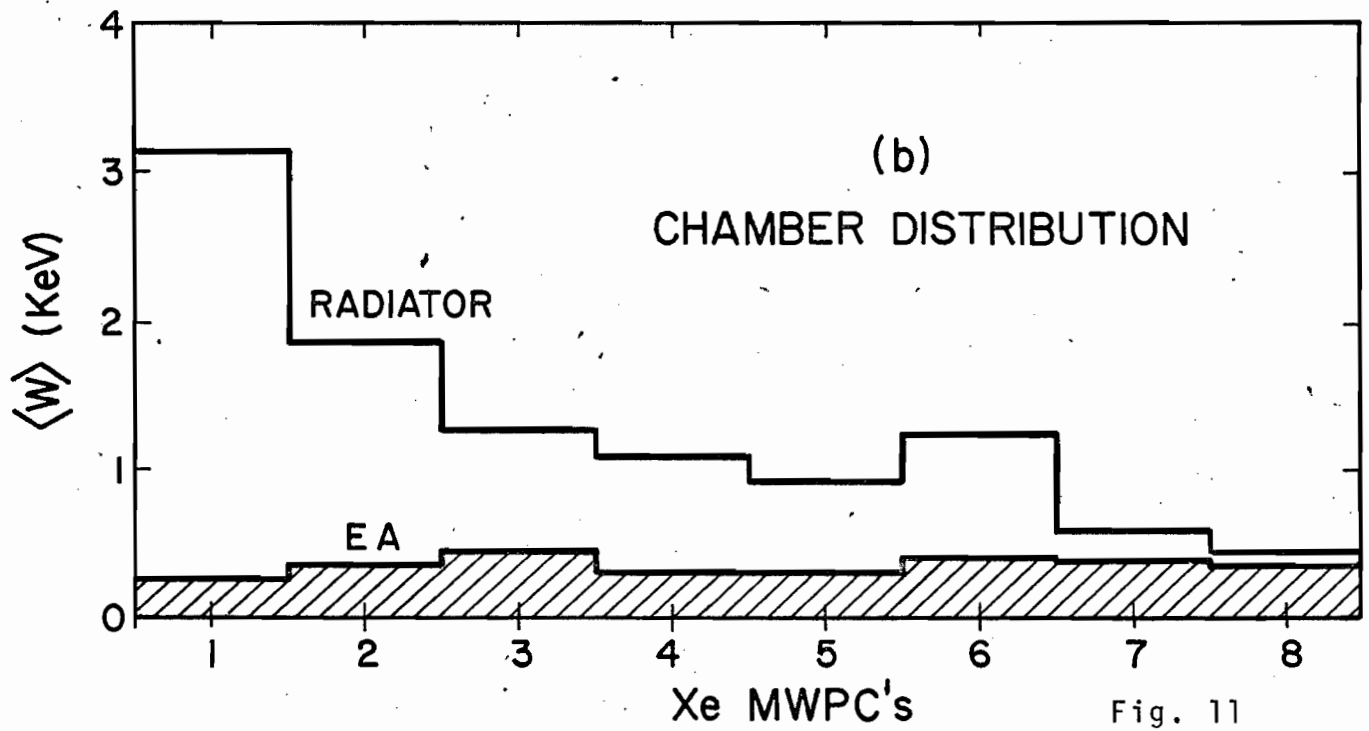
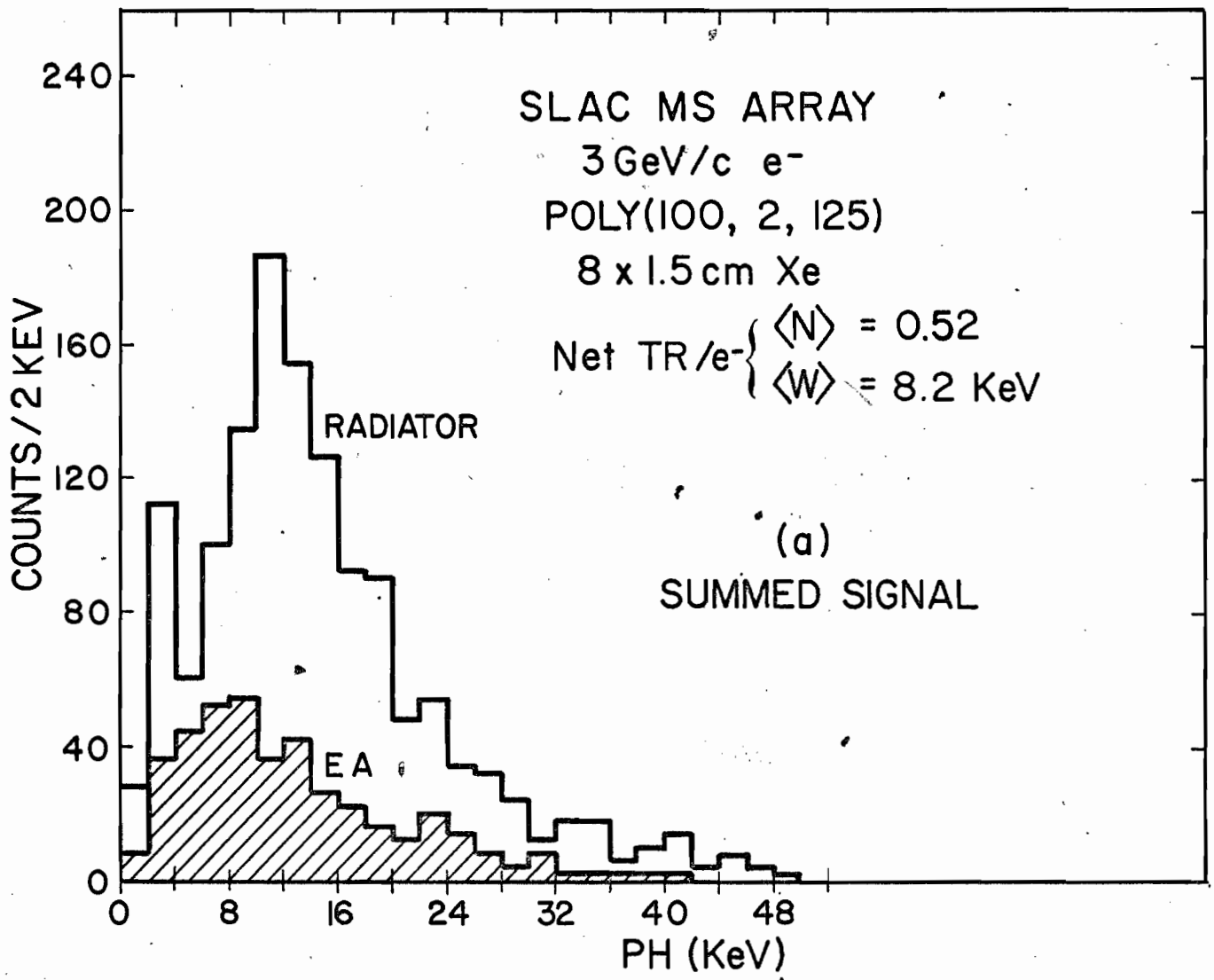


Fig. 11

K<sub>α</sub> SEMI-LOGARITHMIC 46 6213  
5 CYCLES X 70 DIVISIONS  
MADE IN U.S.A.  
KEUFFEL & ESSER CO.

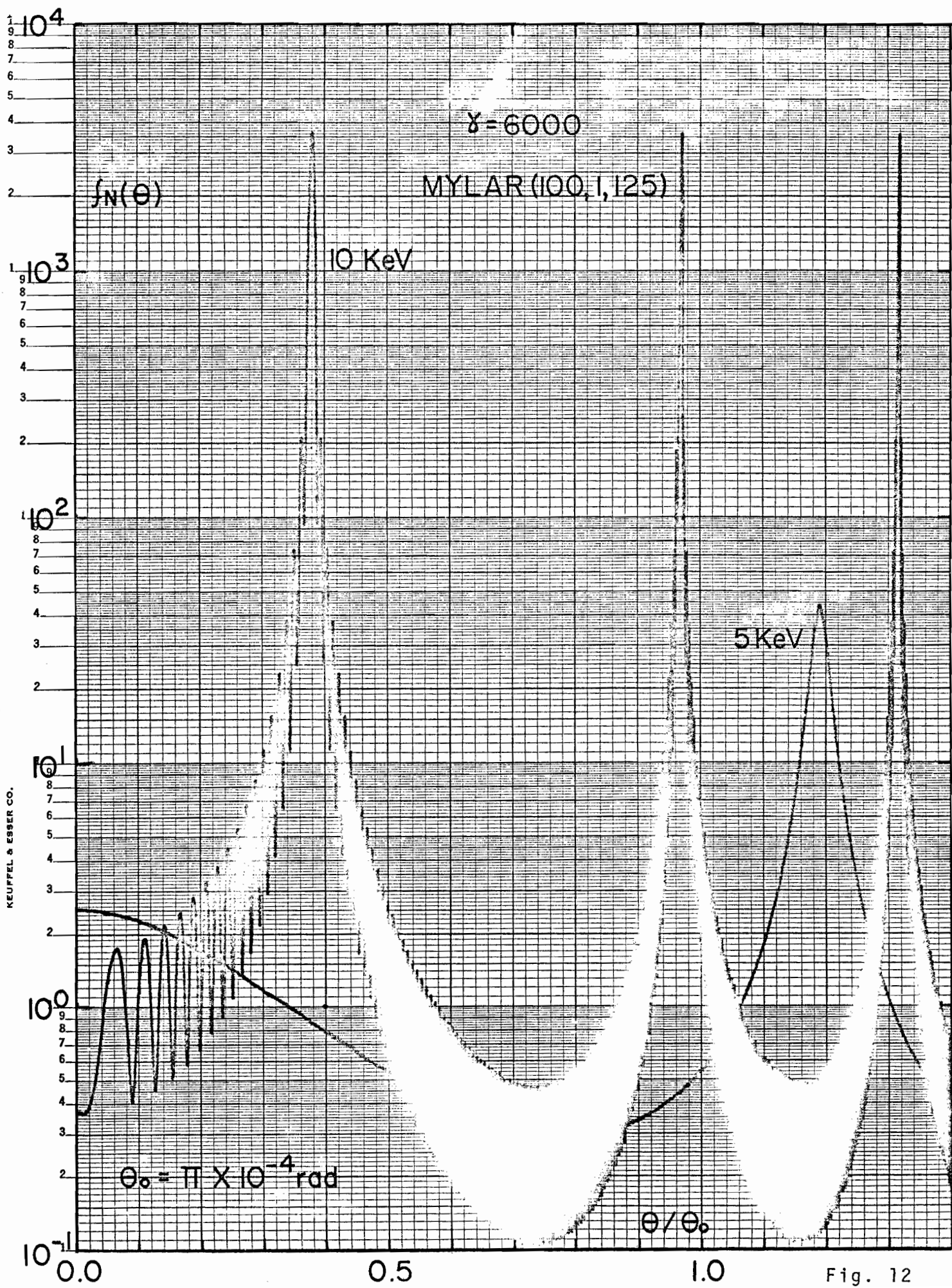


Fig. 12

"A"

57/72

The Experimental Identification of Individual Particles  
by the Observation of Transition Radiation in the X - Ray  
Region

F. Harris, T. Katsura, S. Parker and V.Z. Peterson,  
University of Hawaii.

R.W. Ellsworth and G.B. Yodh,  
University of Maryland.

W.W.M. Allison, C.B. Brooks, J.H. Cobb and J.H. Mulvey,  
Oxford University.

## 1. Introduction

The phenomenon of transition radiation, first predicted by Ginzberg and Frank<sup>(1)</sup> has been explored extensively by Russian groups<sup>(2-5)</sup> and also by Yuan and his collaborators at Brookhaven<sup>(6-9)</sup>. Our intention in the experiment to be described in this report was to study the possibility of using this effect to identify efficiently individual particles of very high  $\gamma$  (i.e.  $\gamma = E/m > 1,000$ ). The results<sup>(10)</sup> confirm the predictions of others<sup>(2, 4, 9, 11)</sup> that individual particles can be identified. The experiment was conducted at the Bevatron in December 1971 using two sets of foil radiators and one set of styrofoam radiators. (see paragraph 2.2). We defer comparison with theoretical predictions of transition radiation yield to a later report, following a more comprehensive series of experiments which will be performed at SLAC this summer. A good review of the theoretical basis is given by Garibian<sup>(5)</sup>.

## 2. The Experiment

### 2.1. Method

The method is to detect the x-rays emitted when a charged particle traverses an interface separating two media of different refractive index, in this case mylar-air. Since the probability of emission is  $\sim \alpha$  per interface the effect must be amplified by the use of many interfaces, such as a series of mylar foils. This is made possible by the fact that the x-rays are highly collimated along the particle trajectory, the typical emission angle being  $\sim 1/\gamma$ .

However, absorption of the x-rays in the foils limits the number of foils that can be effective. In addition, interference between the radiation emitted at the two foil surfaces results in a yield which decreases proportionally to  $t^2$  when  $t$  (the foil thickness) falls below  $t_f$  the "formation zone"<sup>(5)</sup> for the foil material<sup>(12)</sup>.

The compromise between primary yield and absorption leads to an arrangement in which a series of radiators (each consisting of about 100 foils) are interleaved with x-ray detectors (see figure 1). A multiwire proportional chamber (MWPC) is an excellent detector of transition-radiation, especially if filled with a high Z gas such as Krypton or Xenon: the efficiency is good for x-rays in the 3-20 KeV region, the ionization loss by the charged particle is low, the angular acceptance is high and if necessary several contemporaneous particles can be spatially resolved

---

and so separately identified (by virtue of the  $1/\gamma$  emission angle the transition radiation photons remain close to the parent particle trajectory.)

## 2.2. Apparatus.

In this experiment we used 11 MWPC each preceded by radiator stacks containing 100 mylar foils. Two radiator configurations were used: foil thickness,  $t = 1/6$  mil<sup>(13)</sup> and air-spacing,  $d = 60$  mil;  $t = 1/2$  mil with  $d = 30$  mil.

The chambers had a sensitive volume of 20 cm x 20 cm x 1.5 cm and their construction has been described by S. Parker et al<sup>(14)</sup>. For this experiment all the signal-wires were strapped together and one pulse height recorded for each chamber. Two gas fillings were used: 93% Argon + 7% Methane and 93% Krypton<sup>(15)</sup> + 7% Methane. The chamber windows were  $1/4$  mil aluminized mylar.

Data were taken at two values of beam momentum: 1.3 GeV/c and 3 GeV/c. The experimental layout is shown in figure 1. In addition to three beam defining scintillation counters, three Cerenkov counters and a lead-lucite shower counter were used to identify the small percentage of electrons in the negatively charged beam ( $\sim 0.2\%$  at 3 GeV/c and  $\sim 2.2\%$  at 1.3 GeV/c). The  $\pi^-$ -meson contamination of 3 GeV electron triggers was measured to be much less than 1%.

The effect of bremsstrahlung and  $\delta$ -rays produced in the foils was estimated to be negligible. However, to determine background from such processes runs were made in which the radiators were replaced with single sheets of plastic of the same total thickness and also others with no material present.

The charge from each chamber was readout with a preamplifier and sample-and-hold. All eleven chamber signals and the shower counter pulse height were displayed on a CRT to be recorded on 35mm film. In addition the signal from chamber 1, delayed by 200 nsec, was taken direct to the CRT and also displayed so that in the analysis stage all events in which another particle had traversed the system within the integration time of the sample-and-hold ( $\sim 3\mu$  sec) could be excluded. On average  $\sim 12\%$  of recorded events were rejected for this reason; the time distribution of double-pulses indicates that in the worst case less than 4% of the remaining events were unresolved two particle events.

All the data recorded on film was measured by the Oxford PEPR<sup>(16)</sup>, about 80,000 frames in 36 hours.

## 2.3. Energy Calibration

At frequent intervals during the runs each chamber was exposed to an  $\text{Fe}^{55}$  x-ray source (5.9 KeV) and calibration data recorded, also on film.

These measurements showed a systematic variation of the chamber gains with time; all chambers followed the same pattern which had a full excursion of  $\sim 20\%$  over the 24 hours in which most of the data was taken. This effect was probably due to pressure and temperature changes. The  $\text{Fe}^{55}$  data were used to correct for this chamber-independent variation.

In the normal (data taking) mode of readout the trigger was provided by the beam particle selection logic; the  $\text{Fe}^{55}$  x-rays on the other hand had to be self-triggered. When measurements were made taking the output of a single chamber preamplifier directly to a pulse-height-analyser, a different relative pulse-height from  $\text{Fe}^{55}$  x-rays and the peak of the 3 GeV/c  $\pi^-$  ionization loss distribution was obtained. We attribute the difference observed between the two modes to a systematic loss suffered by the signal from  $\text{Fe}^{55}$  x-rays in the self-triggered normal readout due to delays in the trigger circuit. Consequently we have chosen the  $\text{Fe}^{55}$  and 3 GeV/c  $\pi^-$  data taken with the direct readout to a pulse height analyser as the basis of our absolute energy calibration; however we must assign an uncertainty of at most 20% to this calibration procedure.

Although the linearity of chamber response was established beyond the range of interest the readout system (including CRT display) introduced a saturation effect which was not the same in magnitude for all chambers. The saturation level varied between 11.5 KeV and 21 KeV; in figures showing distributions of chamber pulse height all data above the lowest saturation level are shown in one overflow bin.

### 3. Results

#### 3.1 The Distribution of Ionization Loss and the Relativistic Rise

We show in figure 2 A the distribution of ionization loss by 3 GeV/c  $\pi^-$  - mesons in a single Argon + Methane filled chamber (data taken without radiators); figure 2B shows the distribution obtained when the signals from 11 chambers are summed. The curves are the predictions of Blunck and Leisegang (17). As observed by others (18, 19, 20) the experimental distribution is narrower than the Blunck-Leisegang theory for the single chamber, but agreement is reasonable for the "sum of 11" if the system is treated as a single chamber of thickness  $11 \times 1.5$  cms (21). Figures 3A and 3B show the same distributions for 3 GeV/c electrons. Our widths (FWHM) agree well with the data of West (22).

The data show the presence of the relativistic rise. Figure 4 shows our measurements of the relative most-probable energy loss, for both  $\pi^-$  - mesons and electrons, in a single chamber filled with Argon + Methane and also Krypton

+ Methane. The curves are predictions from Sternheimer and Peierls<sup>(23)</sup> and the data are normalised to them at the 3 GeV/c  $\pi^-$  points (there is no density-effect correction for  $\pi^-$  - meson momenta below  $\sim 14$  GeV/c). For 3 GeV/c  $\pi^-$  - mesons ( $\gamma = 21.6$ ) the Sternheimer and Peierls prediction of most-probable energy loss per chamber with Argon + Methane filling is 2.3 KeV compared with our measured value of  $(2.2 \pm 0.1)$  KeV; the corresponding figures for Krypton + Methane are 4.3 KeV and  $(4.2 \pm 0.2)$  KeV. But these values are subject to an uncertainty in energy calibration of up to 20% (see paragraph 2.3). Other data are given in Table I; in agreement with other experiments<sup>(20)</sup> these results suggest that the plateau reached by the ionization loss at large  $\gamma$  is not as high as is predicted by Sternheimer and Peierls.

### 3.2 Transition Radiation

When 3 GeV/c electrons pass through the system with the  $\frac{1}{2}$  mil. mylar radiators in place the single chamber pulse-height distribution obtained is the histogram shown in figure 5A. By comparison with figure 3A, obtained without radiators (actually equivalent absorber and no absorber data combined), it is clear that there is an additional source of energy deposition; this we ascribe to transition radiation.

The with and without-radiator distributions can be compared quantitatively in the following way. Self-absorption in the foils effectively removes all photons of less than 3 KeV, also in Argon there are few examples of ionization loss less than 1 keV per chamber; therefore almost none of the pulses less than 4 keV should be associated with a transition radiation photon - this part of the distribution is 'pure' ionization energy loss. So we can match the shapes of the no-radiator and with-radiator distributions below 4 keV; this has been done by normalising to the same number of events in the 1  $\rightarrow$  3 keV interval. The result is the shape marked by dots superposed on the histogram of figure 5A; this then also shows the number of 'pure' ionization loss signals above 3 keV. In fact the ionization-loss shape follows the histogram well up to about 4.5 keV, confirming that there are very few photons of energy less than  $\sim 3$  keV, entering the chambers.

As the average number of transition radiation photons detected in each chamber is less than one we can estimate a lower limit to the number of detected photons,  $N_\gamma$ , from the number of pulses in excess of the ionization-loss shape. The result is  $3.6 \pm 0.7$  summed over all 11 chambers per incident electron; the error is mainly due to systematic effects, such as relative calibrations, but is not affected by the energy saturation in the readout system. Figure 5B shows the data for Krypton filling with its greater efficiency for photon

detection; in this case  $N_{\gamma} = 5 \pm 0.5$ .

The figures for  $N_{\gamma}$  and also total energy deposition for different radiator configurations and momenta are summarised in Table II. The effect of saturation is that the mean energies given in Table II are systematically low. Using information from the channels with highest saturation and assuming a linear fall off above the saturation point, an estimate of the error has been made; this varies from 2-3% for the  $\pi$ -meson data to a shift in the mean of about 10% for the electron data in Krypton with  $\frac{1}{2}$  mil. radiators.

Table II includes two sets of data, rows 1 and 6, for which no transition radiation effect should be observed. Row 1 is for 3 GeV/c mesons passing through the  $\frac{1}{2}$  mil. radiators and row 6 gives data for 3 GeV/c electrons passing through equivalent absorbers consisting of single sheets of plastic 50 mil. thick. In neither case is a significant effect observed. The values of  $N_{\gamma}$  and energy deposited by transition-radiation photons for 1 and 6 can be taken as indicating the uncertainties in the determination of these quantities. This perhaps suggests that the assigned errors, which are based on an estimated 5% uncertainty in relative calibration of runs made at different times, are conservative.

The yield from 1/6 mil. foils is significantly lower than that for  $\frac{1}{2}$  mil. foils. This thickness dependence, already observed by Yuan, et al<sup>(7)</sup>, is related to the coherence between the radiation from the leading and trailing interfaces of the foil and the observed drop in yield is in reasonable agreement with that expected when the thickness falls below the value of the formation zone.

The one run (row 8, Table II) made with slabs of 2" thick Styrofoam as radiators confirms earlier reports<sup>(2,9)</sup> that transition radiation is generated in this material; in this case the yield was about half that obtained with 100  $\frac{1}{2}$  mil. mylar foils as radiator.

Row 7 in Table II gives results obtained when the  $\frac{1}{2}$  mil. foils were tilted at an angle of  $30^{\circ}$  to the incident 3 GeV/c electron beam. The result is close to that obtained for normal incidence (row 3).

Figure 6 shows three distributions of the sum of pulse heights from all eleven chambers filled with Argon + Methane. On the left is that for 3 GeV/c  $\pi^{-}$  - mesons, on the right and shaded is that for 3 GeV/c electrons passing through the  $\frac{1}{2}$  mil. radiators and the one in the middle is for 3 GeV/c electrons without radiators. The difference between  $\pi^{-}$  - mesons and electrons (no radiators) due to the relativistic rise is clear, as also is the upward shift of the electron with radiators distribution due to transition radiation.

Figure 7 shows the corresponding distributions for Krypton + Methane in the chambers. These are a further demonstration of the greater efficiency of Krypton for the detection of photons, associated with the K absorption edge

at 14.3 keV. The results show a significant relative displacement of the distributions for electrons with, and without radiators and suggest that particle identification is possible by the detection of transition-radiation in the presence of ionization loss.

#### ACKNOWLEDGEMENTS

The authors are grateful to Dr. J.G. Loken for writing the programme to measure the film on the Oxford PEPR. They also wish to thank the staff of the Bevatron and Lawrence Berkeley Laboratory for their aid and hospitality. Dr. M.L. Stevenson is thanked for his assistance in the early stages of the experiment. Several discussions with members of the Brookhaven group working on transition radiation have been very useful.

The A.E.C. (Hawaii), N.S.F. (Maryland) and the R.H.E.L. (Oxford) are thanked for financial support.

REFERENCES AND FOOTNOTES

1. V.L. Ginzberg and I.M. Frank, JETP 16 15 (1946)
2. A.I. Alikhanian, K.M. Avakina, G.M. Garibian, M.P. Lorikian and K.K. Shikhliarov, P.R.L. 25 635 (1970).
3. A.I. Alikhanian, K.A. Ispirian, A.G. Oganessian and A.G. Tamanian, N.I.M. 89 147 (1970).
4. A.A. Franghian, F.R. Haratjunian, G.A. Hekimian, A.A. Nasarian and G.B. Torgomian, P.L. 34B 227 (1971).
5. G.M. Garibian, Yerevan pre-print EØN-TØ-13 (1970). This article contains references to many other papers on transition radiation.
6. L. Yuan, C.L. Wang and S. Prunster, PRL 23 496 (1969).
7. L. Yuan, C.L. Wang, H. Uto and S. Prunster, PRL 25 1513 (1970).
8. L. Yuan, C.L. Wang, H. Uto and S. Prunster, P.L. 31B 603 (1970).
9. H. Uto, L. Yuan, G. Dell and C.L. Wang, N.I.M. 97 389 (1971)
10. These results were presented in preliminary form at the American Physical Society meeting, Washington, April 1972.
11. R.W. Ellsworth, J. MacFall, P.K. MacKeown and G.B. Yodh, Proceedings of the 6th Inter-American Seminar on Cosmic Radiation La Paz, Bolivia 2 344 (1970).
12.  $t_f$  is a function of  $\gamma$ , the energy and angle of emission of the photon and the foil plasma frequency; for example the value of  $t_f$  for emission of 10 keV photons at an angle of  $\frac{1}{\gamma}$  (the peak of the angular distribution) by a particle of  $\gamma = 6,000$  entering mylar is  $\sim \frac{1}{4}$  mil.<sup>(13)</sup>
13. 1 mil. equals  $10^{-3}$  inch.
14. S. Parker, R. Jones, J. Kadyk, M.L. Stevenson, T. Katsura, V.Z. Peterson and D. Yount, N.I.M. 97 181 (1971).
15. Although Krypton is radioactive (since atmospheric testing of nuclear bombs introduced fission products) this is not a problem in this experiment since data is taken in coincidence with beam defining counters.
16. J.P. Berge, C.B. Brooks, P.G. Davey, J.F. Harris and J.G. Loken "Proceedings of the Second International Colloquim on PEPR" M.I.T., Cambridge, Mass. May 1970.
17. O. Blunck and S. Leisegang, Zeits. für Phys. 128 500 (1950)
18. G. Knop, A. Minten and B. Nellen, Zeits. für Phys. 165, 533 (1961)
19. Z. Dimcovski, J. Favier, G. Charpak and G. Amato, N.I.M. 94 151 (1971)
20. P.V. Ramana Murthy, N.I.M. 63 77 (1968).
21. The parameter  $b^2$ , defined by Blunck and Leisegang<sup>(17)</sup>, has the value  $\sim 164$  for 3 GeV/c  $\pi^-$  mesons crossing a single chamber, and  $\sim 15$  for a chamber of thickness eleven times this.

22. D. West, Proc. Roy. Soc. A66, 306 (1953)
23. R. Sternheimer and R.F. Peierls, Phys. Rev. B3 3681 (1971)

TABLE 1 IONIZATION ENERGY LOSS

CHAMBER GAS	MOMENTUM AND PARTICLE	$\gamma$	MEASURED MOST-PROBABLE ENERGY LOSS PER CHAMBER (SUBJECT TO $\sim$ 20% CALIBRATION UNCERTAINTY) (KeV)*	FULL- WIDTH- HALF- MAXIMUM (KeV)*	RELATIVE MOST-PROBABLE IONIZATION ENERGY-LOSS PER CHAMBER (NORMALISED TO STERNHEIMER-PEIERLS <sup>(23)</sup> ) ( FOR 3 GeV/c $\pi$ -MESON )	
					EXPERIMENT	PREDICTION
ARGON	1.3 GeV/c $\pi^-$	9.4	$1.9 \pm 0.1$	2.0	$1.07 \pm 0.07$	1.11
	3.0 GeV/c $\pi^-$	21.6	$2.2 \pm 0.1$	2.1	1.24	1.24
	1.3 GeV/c $e^-$	2,550	$2.9 \pm 0.2$	2.6	$1.64 \pm 0.14$	1.77
	3.0 GeV/c $e^-$	5,880	$2.9 \pm 0.2$	2.4	$1.64 \pm 0.14$	1.78
KRYPTON	3.0 GeV/c $\pi^-$	21.6	$4.2 \pm 0.2$	3.3	1.26	1.26
	3.0 GeV/c $e^-$	5,880	$5.7 \pm 0.3$	4.5	$1.71 \pm 0.13$	1.87

\* See paragraph 2.3; the overall 20% uncertainty in energy calibration is not included in the errors given.

TABLE II TRANSITION RADIATION

Momentum Particle	G A S	Radiator	$\gamma$	11 Chamber Totals/ Incident Particle (KeV)*				
				Lower Limit No. of detected Photons	Lower Limit Total Energy Deposition	Ionization Loss Energy Deposition	Lower Limit Transition Radiation Energy Deposition	
1 3.0 GeV/c $\pi$	A R G O N	100, $\frac{1}{2}$ mil	21.6	$0.3 \pm 1$	$36.5 \pm 1.8$	$35.2 \pm 1.8$	$1.3 \pm 2.5$	
2 1.3 GeV/c $e^-$		"	2,550	$2.5 \pm 0.8$	$57.5 \pm 2.8$	$45.0 \pm 2.2$	$12.5 \pm 3.6$	
3 3.0 GeV/c $e^-$		"	"	5,880	$3.6 \pm 0.7$	$70.0 \pm 3.5$	$48.6 \pm 2.4$	$21.4 \pm 4.1$
4 1.3 GeV/c $e^-$		100, $\frac{1}{6}$ mil	2,550	$1.0 \pm 1.0$	$51.6 \pm 2.5$	$45.0 \pm 2.2$	$6.6 \pm 3.3$	
5 3.0 GeV/c $e^-$		"	"	5,880	$2.0 \pm 0.8$	$56.6 \pm 2.8$	$48.6 \pm 2.4$	$8.0 \pm 3.7$
6 3.0 GeV/c $e^-$		1,50 mil	5,880	$0.3 \pm 1$	$48.5 \pm 2.4$	$47.0 \pm 2.3$	$1.5 \pm 3.2$	
7 3.0 GeV/c $e^-$		(100, $\frac{1}{2}$ mil (tilted $30^\circ$ )	5,880	$3.3 \pm 0.7$	$67.6 \pm 3.3$	$48.6 \pm 2.4$	$19.0 \pm 4.1$	
$\beta$ 3.0 GeV/c $e^-$		2" styrofoam	5,880	$1.4 \pm 1$	$57.5 \pm 2.8$	$48.6 \pm 2.4$	$8.9 \pm 3.7$	
9 3.0 GeV/c $e^-$	K R Y P T O N	100, $\frac{1}{2}$ mil	5,880	$5.0 \pm 0.5$	$122 \pm 6.1$	$85.6 \pm 4.2$	$36.4 \pm 7.4$	
10 3.0 GeV/c $e^-$		100, $\frac{1}{6}$ mil	5,880	$2.6 \pm 0.7$	$100 \pm 5.0$	$85.6 \pm 4.2$	$14.4 \pm 6.5$	

\* See paragraph 2.3; there is an overall 20% uncertainty in energy calibration which is not included in the errors given.

## Figure Captions

### Figure 1

Diagram of beam and transition radiation detector.

### Figure 2A

Distribution of ionization energy loss in a single chamber for 3 GeV/c  $\pi^-$  - mesons. The curve shows the predictions of Blunck and Leisegang<sup>(17)</sup>. The chamber thickness is  $2.5 \cdot 10^{-3} \text{ gm cm}^{-2}$  and the gas 93% Argon and 7% Methane.

### Figure 2B

Distribution of ionization energy loss for 3 GeV/c  $\pi^-$  - mesons when signals from eleven chambers are added. The curve is the Blunck and Leisegang prediction treating the system as one chamber of thickness  $27.3 \cdot 10^{-3} \text{ gm cm}^{-2}$  containing 93% Argon and 7% Methane.

### Figure 3A

Distribution of ionization energy loss for 3 GeV/c electrons in single chamber containing 93% Argon and 7% Methane. The curve is the Blunck and Leisegang prediction.

### Figure 3B

Distribution of sum of eleven chambers for ionization loss by 3 GeV/c electrons. The curve is the Blunck and Leisegang prediction treating the system as one chamber of thickness  $27.3 \cdot 10^{-3} \text{ gm cm}^{-2}$  containing 93% Argon and 7% Methane.

### Figure 4

Relative most probable energy loss as a function of the ratio momentum/mass. Points marked  $\odot$  are for 93% Argon + 7% Methane, and those marked  $\circ$  are for 93% Krypton + 7% Methane. The curves have been calculated from Sternheimer and Peierls<sup>(23)</sup>. The relative ionization has been normalised to the calculated values at the points corresponding to the 3 GeV/c  $\pi^-$  - meson data (there is no density correction for  $\pi^-$  - meson momenta below  $\sim 14 \text{ GeV/c}$ ).

### Figure 5A

Distribution of energy deposited in a single Argon/Methane filled chamber when 3 GeV/c electrons pass through the  $\frac{1}{2}$  mil. mylar radiators. The points marked with a dot show the distribution obtained without radiators when this is normalized to have equal area in the 1 keV to 3 keV region.

### Figure 5B

As for 5A but for chambers filled with 93% Krypton + 7% Methane. The

dotted distribution has been normalised to equal the histogram area in the 2-5 keV region.

Figure 6

This shows the distributions of total energy deposited in 11 chambers plotted with equal areas for the three cases: 3 GeV/c  $\pi^-$  - mesons, 3 GeV/c electrons without radiators, and 3 GeV/c electrons with  $\frac{1}{2}$  mil. radiators; chamber gas 93% Argon and 7% Methane. Saturation in some of the readout channels causes a systematic underestimate of the number of large values.

Figure 7

As for Figure 6 but with a gas mixture of 93% Krypton + 7% Methane.

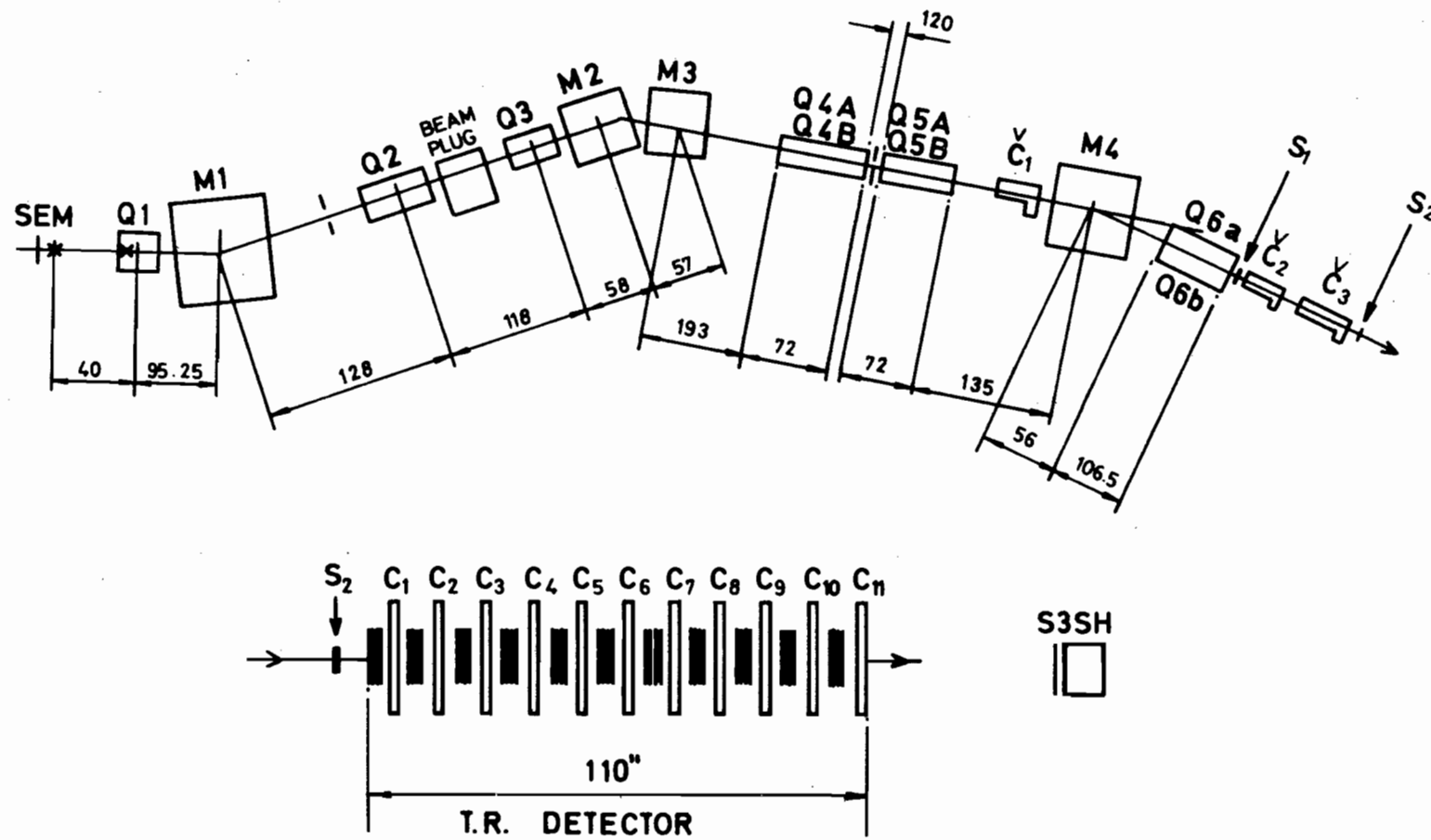


Fig. 1

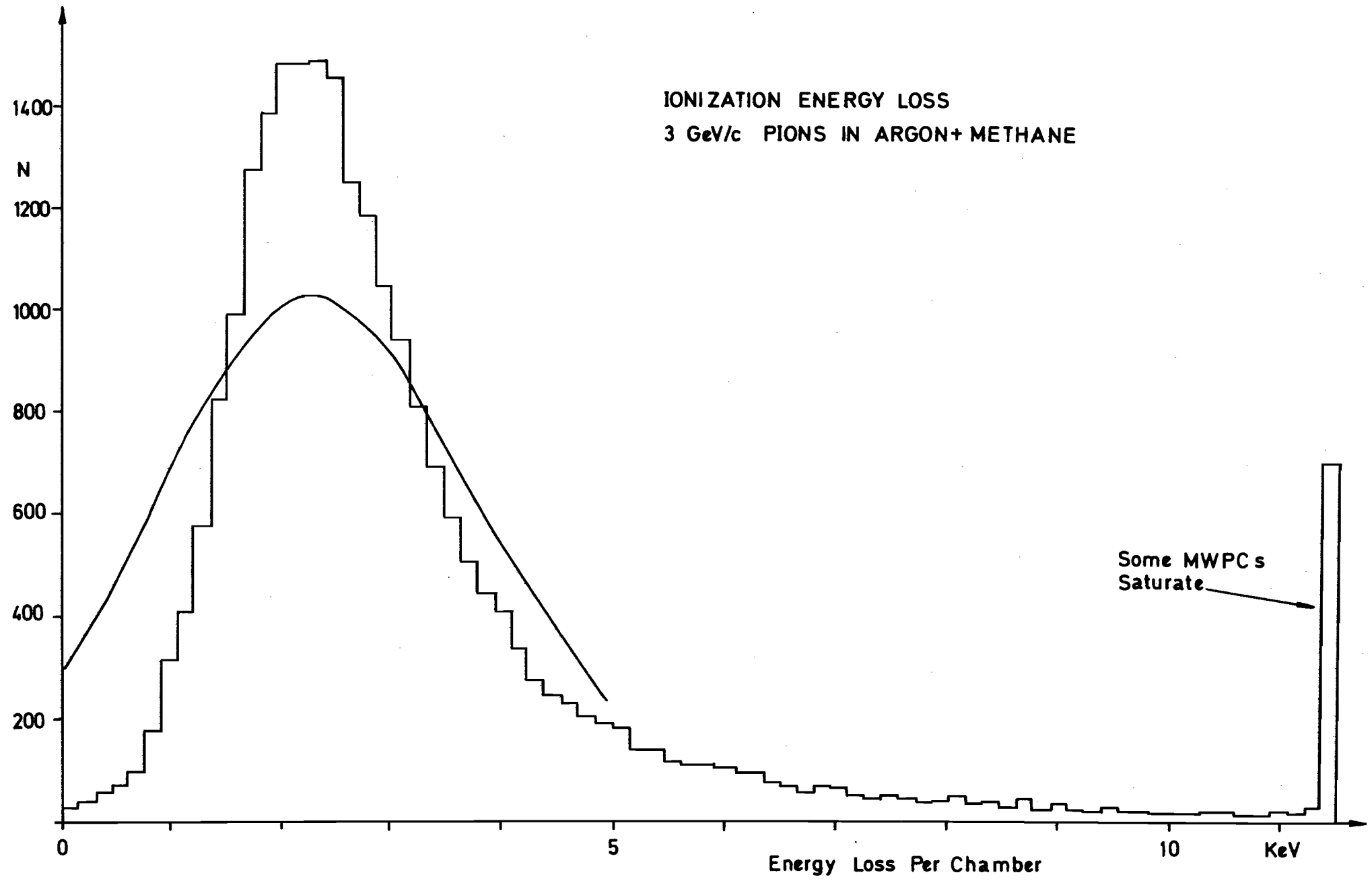


Fig. 2A

IONIZATION ENERGY LOSS IN 11 CHAMBERS  
3 GeV/c PIONS IN ARGON + METHANE  
(WITHOUT SATURATION CORRECTION)

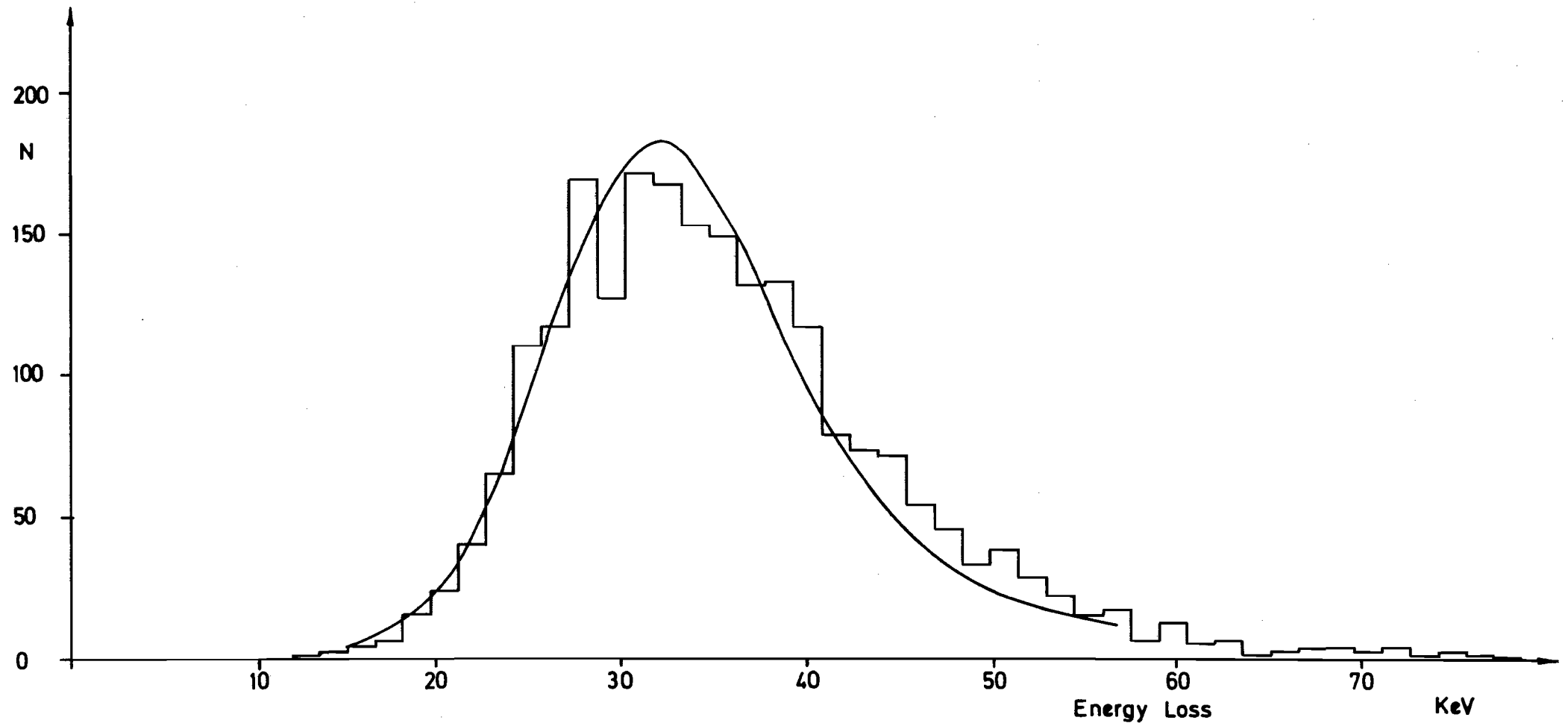


Fig. 2 B

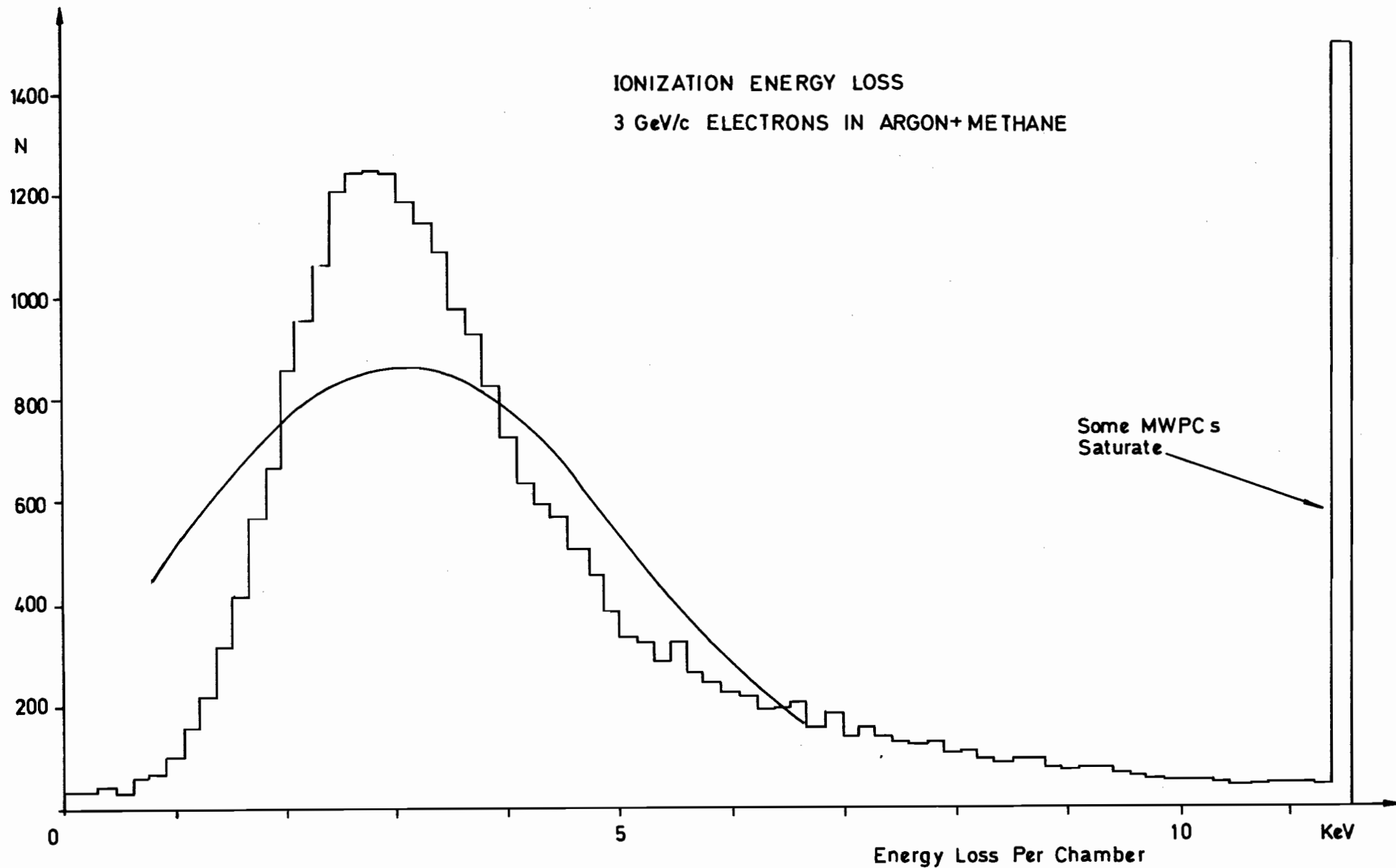


Fig. 3A

IONIZATION ENERGY LOSS IN 11 CHAMBERS  
3 GeV/c ELECTRONS IN ARGON + METHANE  
(WITHOUT SATURATION CORRECTION)

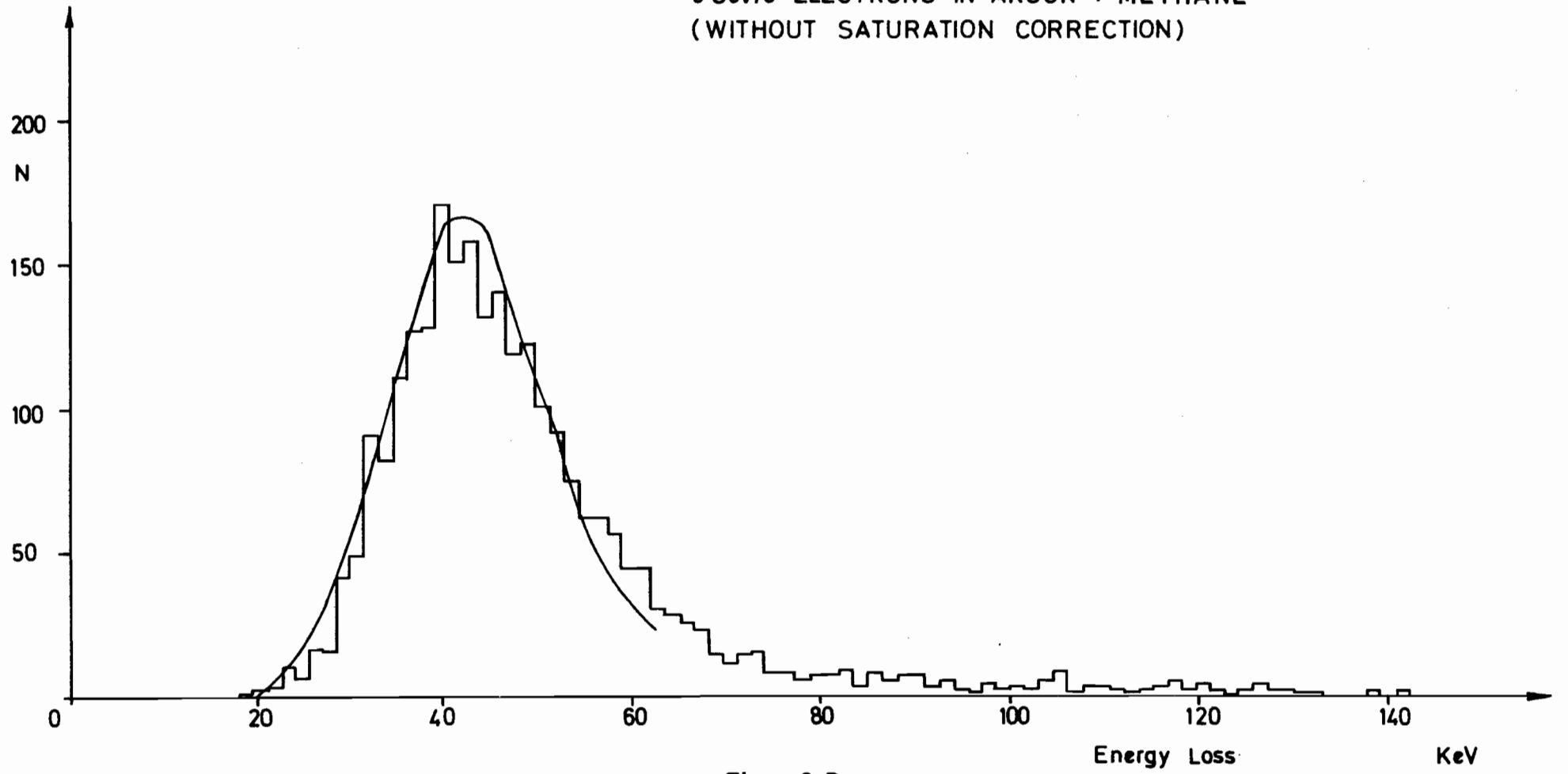


Fig. 3 B

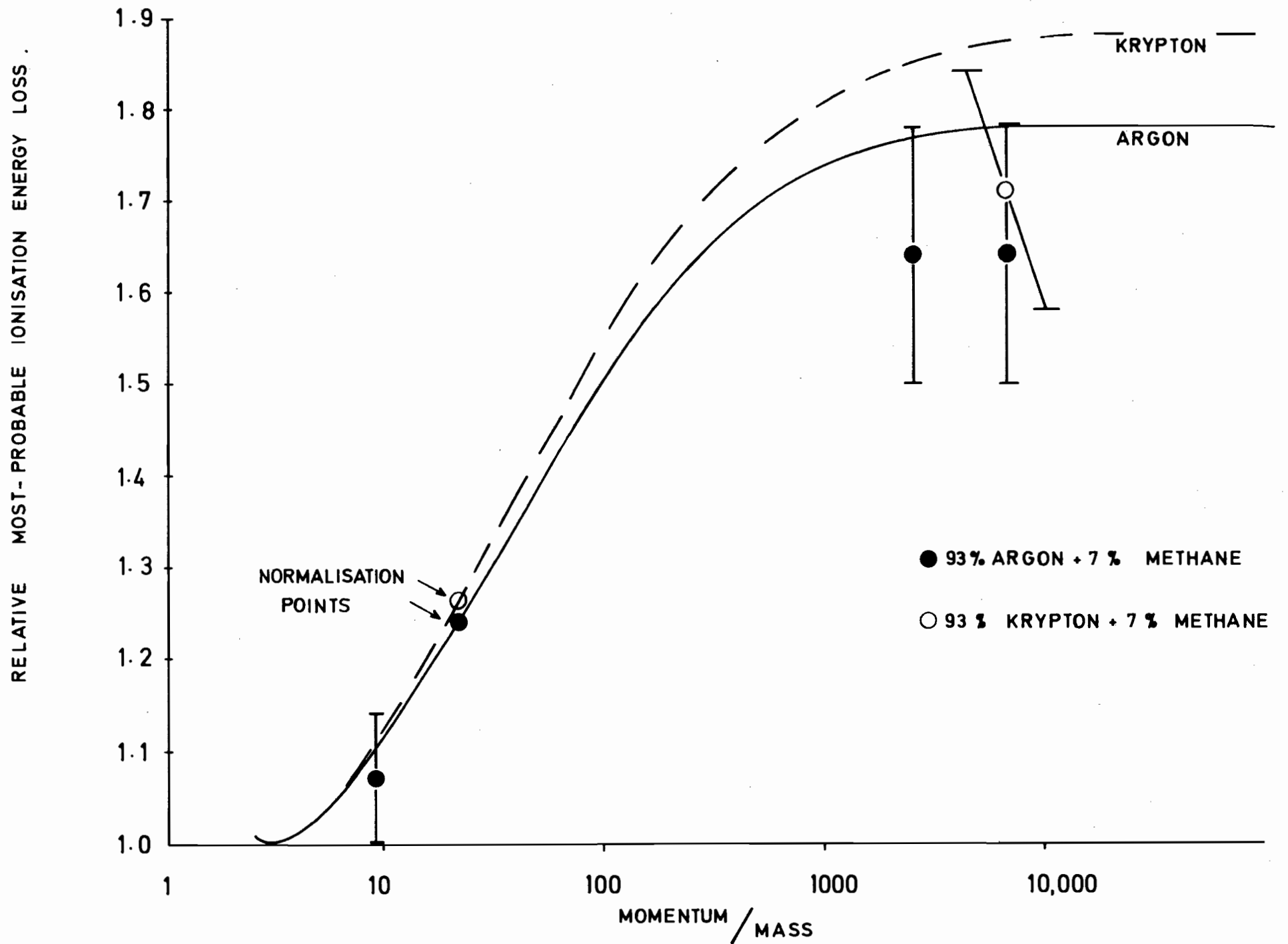


Fig. 4

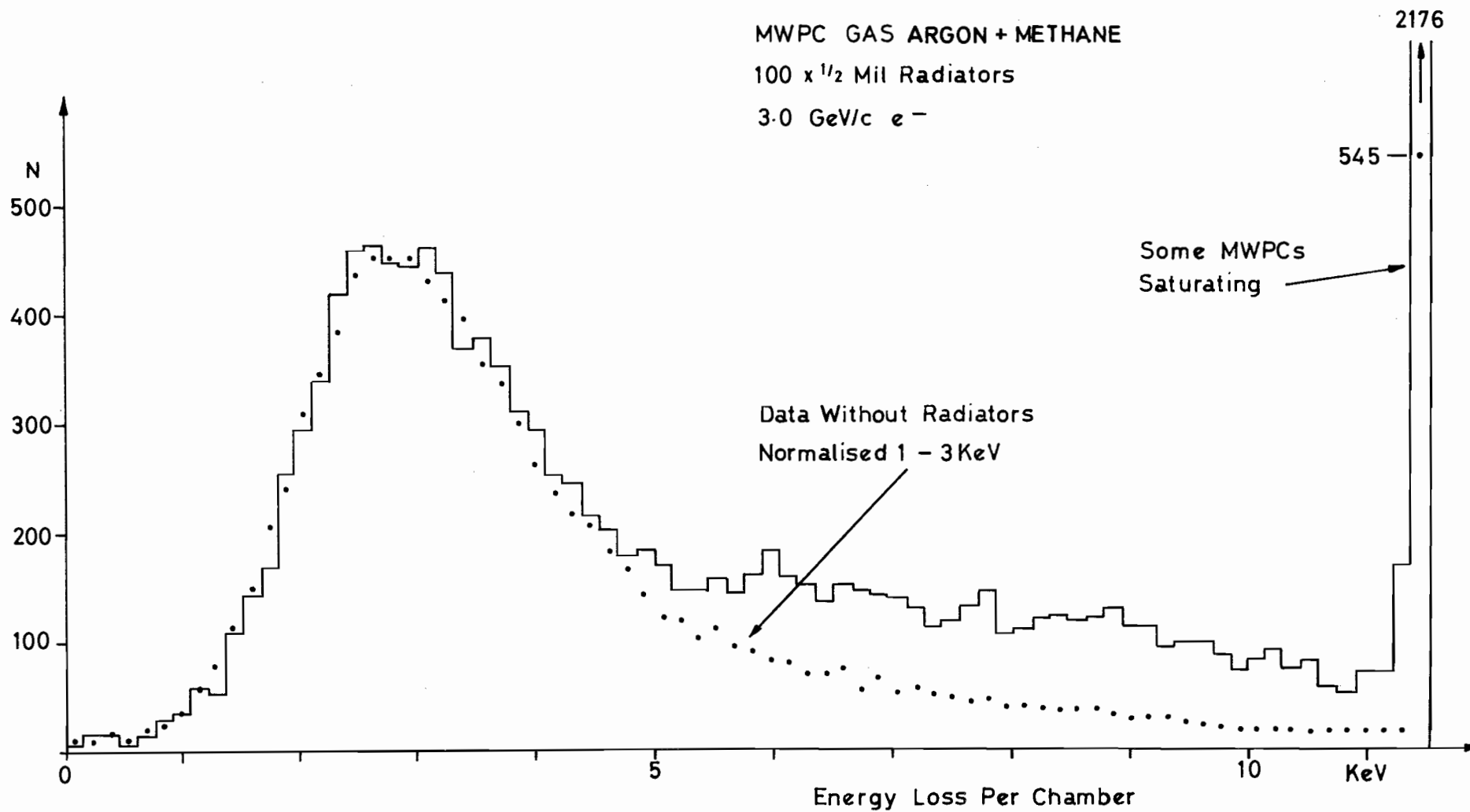


Fig. 5 A

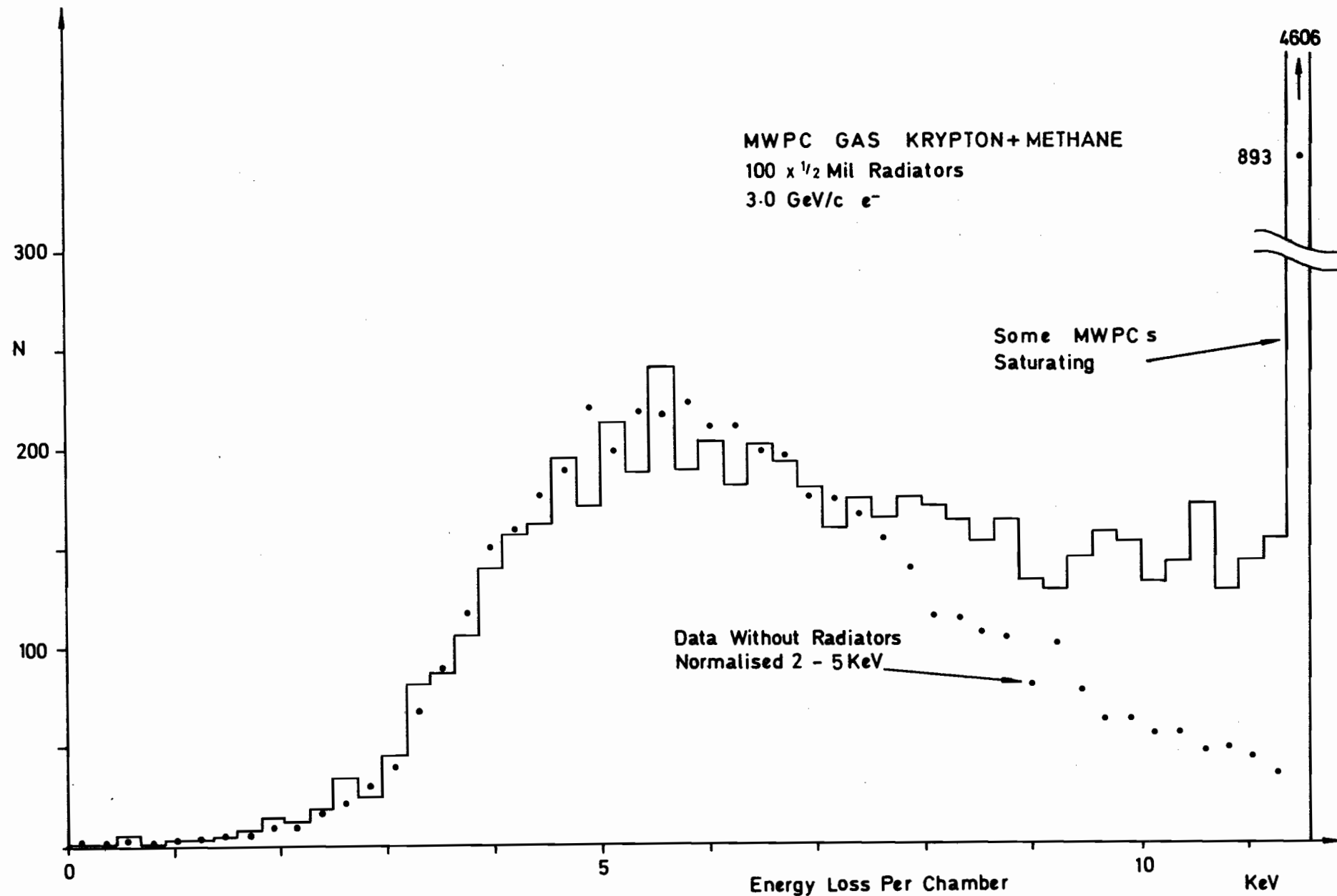


Fig. 5 B

EQUAL AREA SPECTRA OF ENERGY LOSS  
IN 11 CHAMBERS (ARGON + METHANE)  
(WITHOUT SATURATION CORRECTION)

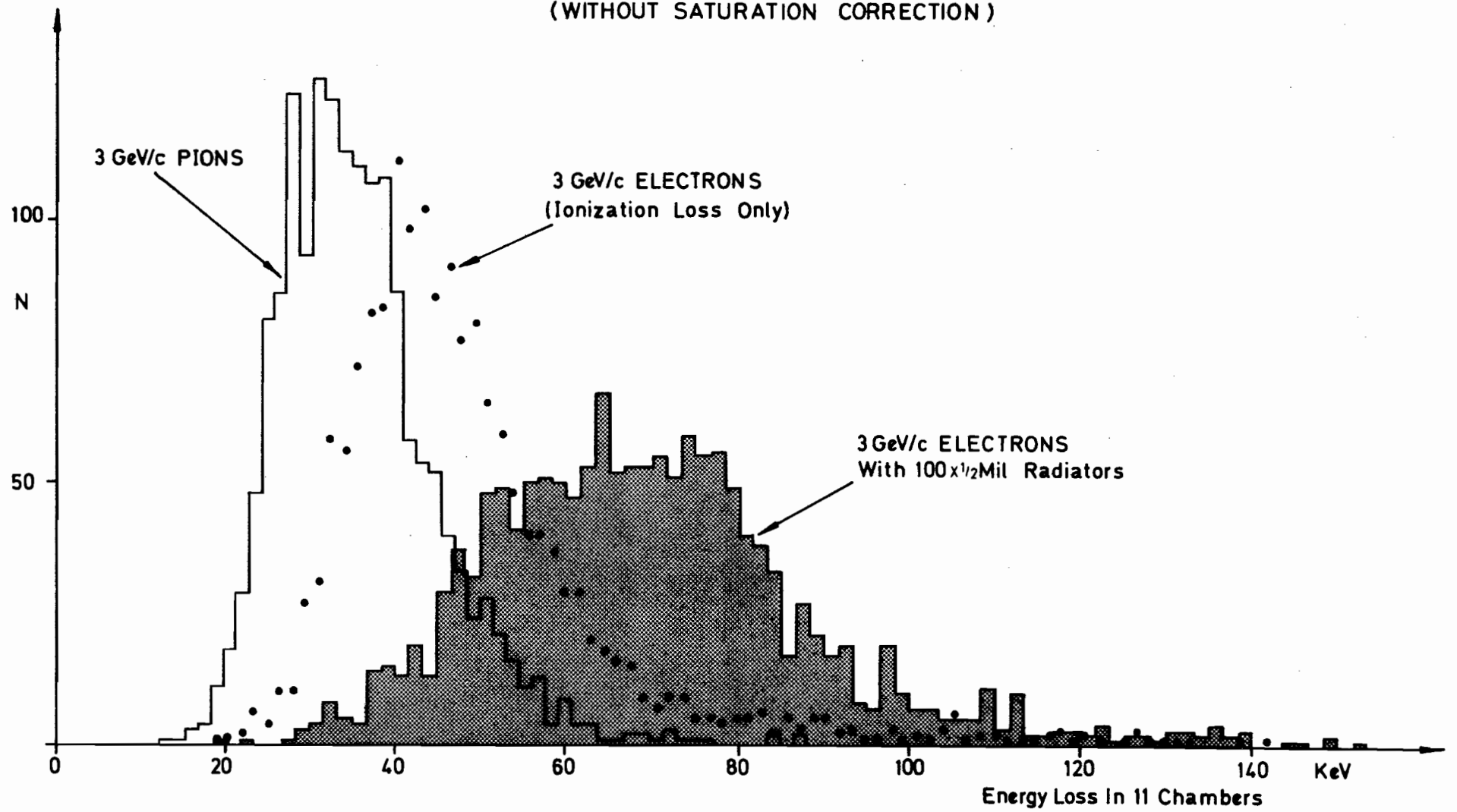


Fig. 6

EQUAL AREA SPECTRA OF ENERGY LOSS  
IN 11 CHAMBERS ( KRYPTON + METHANE )  
( WITHOUT SATURATION CORRECTION )

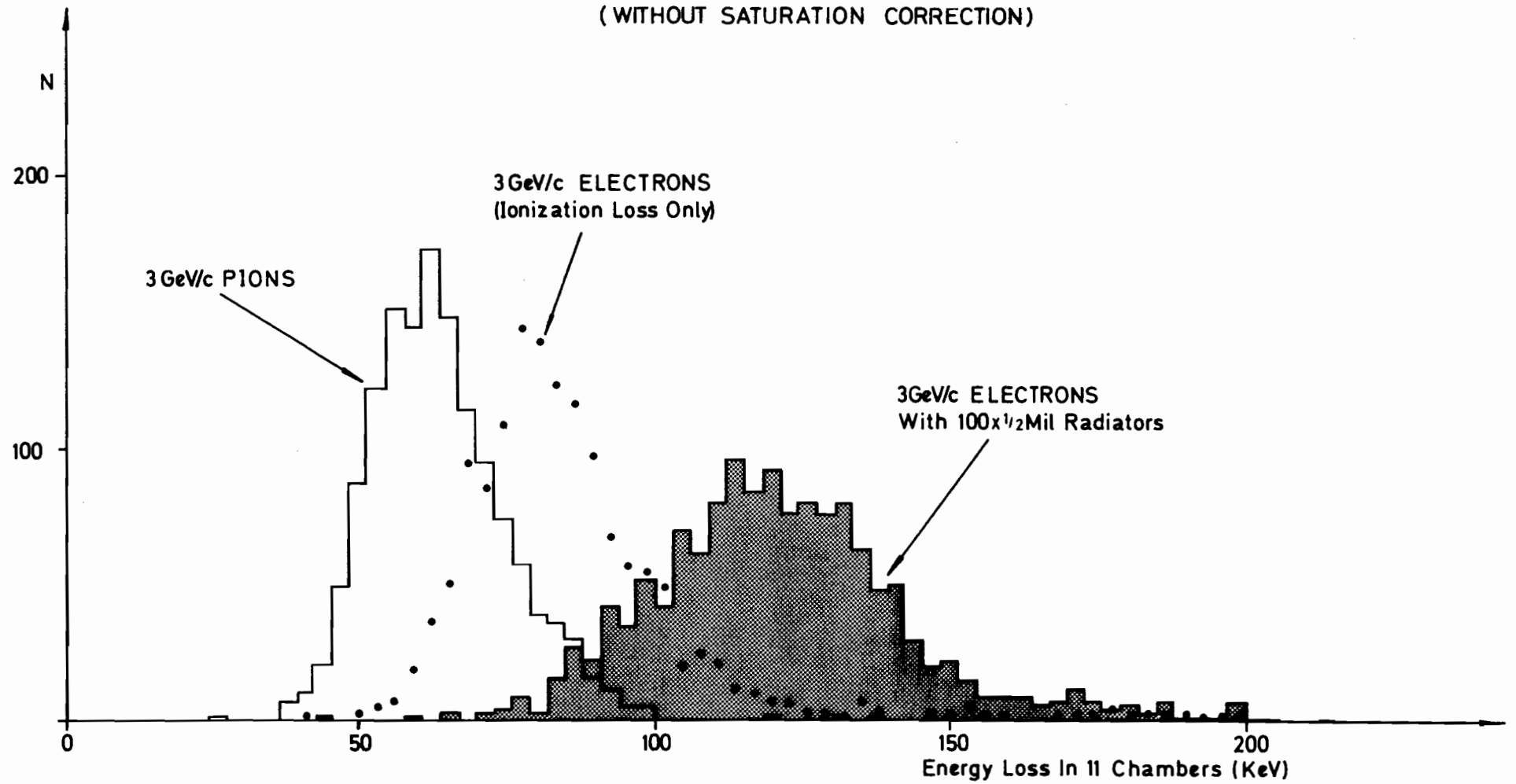


Fig. 7

Transition Radiation and  
Particle Identification\*

Sherwood I. Parker\*\*

High Energy Physics Group

University of Hawaii

Honolulu, Hawaii

(Summary of invited paper given in the Instrumentation  
Session at the XVith International Conference on  
High Energy Physics, Chicago, USA, on September 7, 1972).

\* Work supported in part by the U. S. Atomic Energy Commission  
under contract AT(04-3)-511.

\*\* Presently located at Lawrence Berkeley Laboratory, University  
of California, Berkeley, California.

## Transition Radiation and Particle Identification

Transition radiation is produced when a charged particle passes an interface between two media of different dielectric constants. Consider, for example, a charged particle approaching a homogeneous dielectric foil:

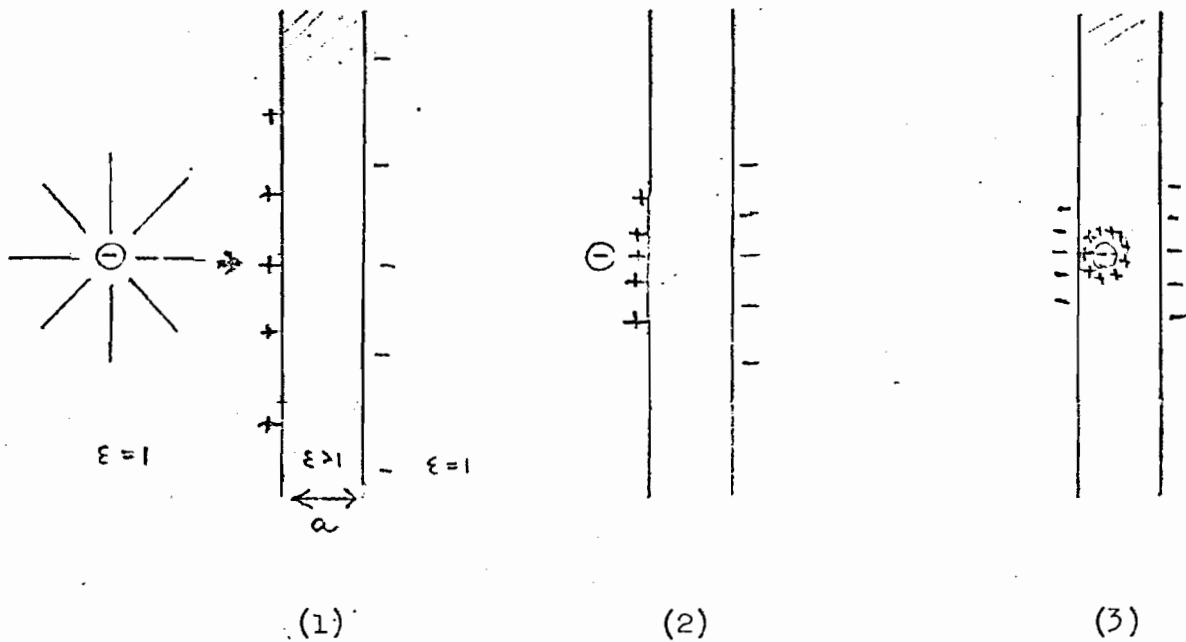
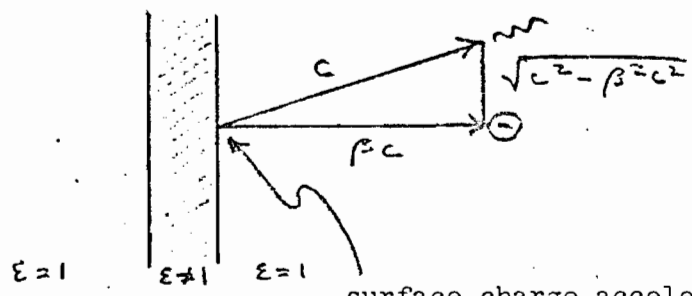


Fig. 1

The processes shown above reverse as the particle leaves the foil. It is clear that charges on the surface are being accelerated and will radiate. As the incident particle becomes relativistic and its electric field becomes compressed in the transverse plane, the motion and resultant radiation extend to ever higher frequencies, and the total energy radiated increases nearly in proportion to  $\gamma$ .

Since the radiation leaving the foil travels with velocity  $c$  and the particle with velocity  $\beta c \approx c$ , the angle of maximum intensity is nearly straight forward:

$$\theta_{\text{peak}} \approx \sin \theta_{\text{peak}} \approx \frac{\sqrt{c^2 - \beta^2 c^2}}{c} = \frac{1}{\gamma} \quad (1)$$



surface charge accelerated near point of emergence of particle

Fig. 2

Unlike Cerenkov radiation, transition radiation is generated whenever  $\epsilon \neq 1$ , including the important X-ray region where  $\epsilon < 1$ .

Transition radiation was first predicted by Ginzburg and Frank in 1946<sup>1</sup> and found by Goldsmith and Jelley in 1959<sup>2</sup>. Lilienfeld also observed it in 1919<sup>3</sup>, but its nature was not recognized at that time. The recent interest in it is largely due to the possibility of using it to measure  $\gamma$ . Then with a momentum or energy measurement ( $\gamma m$ ), highly relativistic particles can be identified through their rest mass. Pioneering work has been done by Russian theorists<sup>1,4</sup> and experimental groups<sup>5</sup> and by the Brookhaven group in the US.<sup>6</sup> We report here the identification of individual particles by the detection of X-ray transition radiation<sup>7</sup>. First, however, we list

Some Useful Formulas

1. Radiation from a perpendicular traversal of a single interface ( $\epsilon_1 \rightarrow \epsilon_2$ ) <sup>8</sup>

$$\frac{d^2W}{d\Omega dE} = \frac{\alpha \beta^2}{\pi^2} \sin^2 \theta \cos^2 \theta \left| \frac{(\epsilon_1 - \epsilon_2)(1 - \beta^2 - \beta \sqrt{\epsilon_1 - \epsilon_2} \sin^2 \theta)}{(1 - \beta^2 \epsilon_2 \cos^2 \theta)(\epsilon_1 \cos \theta + \sqrt{\epsilon_2} \sqrt{\epsilon_1 - \epsilon_2} \sin^2 \theta)(1 - \beta \sqrt{\epsilon_1 - \epsilon_2} \sin^2 \theta)} \right|^2 \quad (2)$$

Here  $\alpha = 1/137$ ,  $\beta = v/c$ ,  $\epsilon_i$  = dielectric constant of medium  $i$ ,  $E = \hbar \omega$

$$\left( \epsilon = 1 - \frac{\omega_p^2}{\omega^2} \quad \text{in the X-ray region, } \omega_p = \text{plasma frequency} = \sqrt{\frac{4\pi N e^2}{m}} \right. \\ \left. \approx \frac{29}{\hbar} \sqrt{\frac{\rho Z}{A}} \text{ electron volts} \right)$$

For  $\beta \rightarrow 1$  this simplifies, in the X-ray region to

$$\frac{d^2W}{d\Omega dE} = \frac{\alpha}{\pi^2} \theta^2 \left| \frac{1}{\gamma^{-2} + \theta^2 + (\omega_1^2/\omega^2)} - \frac{1}{\gamma^{-2} + \theta^2 + (\omega_2^2/\omega^2)} \right|^2 \quad (3)$$

where  $\omega_1$  and  $\omega_2$  are the specific plasma frequencies. We now specialize to solid-gas interfaces and set  $\omega_1 = 0$ ,  $\omega_2 = \omega_p$ .

2. Radiation from a stack of plates. Formulas are given in Ref. 4, but modifications must be made to allow for absorption of the soft X-rays. A computer program is usually needed for useful results.
3. Intergrated radiation from a single surface-vacuum interface

$$W = \frac{1}{3} \alpha \gamma \hbar \omega_p \quad (4)$$

4. Limiting frequency:  $\frac{dW}{dE}$  has dropped to half its low frequency value at

$$\omega_{lim} = \frac{1}{2} \gamma \omega_p, \quad (5)$$

typically in the 10KeV region for NAL energies.

Since typical transition radiation quanta have

$$E \approx \frac{1}{2} \hbar \omega_{lim} = \frac{1}{4} \gamma \hbar \omega_p \quad (6)$$

the total energy divided by the typical energy is

$$\frac{W}{E} = \frac{\frac{1}{3} \alpha \gamma \hbar \omega_p}{\frac{1}{4} \gamma \hbar \omega_p} \approx \alpha$$

$\sim \alpha$  photons are emitted per interface.

(7)

5. Formation zone: two interfaces must be separated by more than about

$z_{\text{formation}} = \frac{2c}{\omega \left( \frac{1}{\gamma^2} + \theta^2 + \frac{\omega_p^2}{\omega^2} \right)}$

(8)

to prevent cancellation of the radiation from the two surface. Referring to the first figure, the cancellation can be seen to come from the identical motion of the + and - charges on the two surfaces as  $a \rightarrow 0$ . Cancellation is prevented by differing radiation and particle paths ( $\theta^2$  term), and by the departure from  $c$  of both the particle velocity ( $1-\beta \propto \frac{1}{\gamma^2}$  term) and the radiation phase velocity ( $\omega_p^2/\omega^2$  term). For example, in the solid (see (6)),

$$\left( \frac{\omega_p}{\omega} \right)^2 \approx \left( \frac{\omega_p}{\frac{1}{4} \gamma \omega_p} \right)^2 = \frac{16}{\gamma^2}$$

and the plasma term dominates the  $\theta^2 (\approx \frac{1}{\gamma^2})$  and the  $\frac{1}{\gamma^2}$  terms,

giving for 400 GeV pions,

$$z_{\text{formation}} \approx \frac{2c}{\omega \left( \frac{\omega_p^2}{\omega^2} \right)} = \frac{2c \left( \frac{1}{4} \gamma \omega_p \right)}{\omega_p^2} \approx \frac{c}{2\omega_p} \gamma \approx 10^{-3} \text{ cm}$$

If the foils are separated by gas or vacuum,  $\omega_p \approx 0$  there and the necessary separation distance is about an order of magnitude larger.

### Radiators

The major fact of life is given by (7) -  $\propto$  photons are generated per interface. Thus typical radiator stacks must have  $\sim 10^2$  foils. The full  $\gamma$  dependence for detected energy will not be realized unless, (1) the detector is sensitive to energies up to  $\sim \gamma \hbar \omega_p$  and, (2), the foil thickness and spacing exceed the corresponding  $z_{\text{formation}}$ . An upper limit to the number and thickness of foils is set however, by the self-absorption of radiation, primarily through the photoelectric effect. Thus, to achieve adequate statistics, it is often necessary to have repeated radiator - detector sets. Because of its narrow angular distribution, the transition radiation must be detected in the presence of ionization from the particle track unless a long drift distance or magnetic separation is used. Both of these are only practical, if repeated radiators and detectors are used, for particle identification in beam lines. Some recent measurements have been taken with crystalline radiators<sup>9</sup>, but most commonly, low Z foils (to reduce photoelectric absorption) of as high a density as possible (to increase  $\epsilon - 1$ ) are used. Beryllium would be ideal, but the usual accommodation with reality normally results in the use of separated Mylar, polyethylene, or aluminum foils. A more compact

( 2mm rather than 200 mm) though less efficient radiator could be constructed of alternate high and low density foils since  $z_{\text{formation}}$  is so much less for solids<sup>10</sup>. Constructive interference effects between separate foils are possible without excessive mechanical tolerances since the near equality of the particle and wave velocities increases the tolerances from  $\Delta z \ll \lambda_{\text{TR}} \sim 1 \text{ \AA}$  to  $\Delta z \ll z_{\text{formation}}$ .

No significant interference effects would be expected with electrons because multiple Coulomb scattering changes their direction by

$\theta_{\text{peak}} \approx \frac{1}{\gamma}$  every few foils. Multiple Coulomb scattering also plays a role in slowing the  $\gamma$  dependence above

$$\gamma \approx 16 L_{\text{radiation}} \frac{\omega_p}{c} \left( \frac{M_{\text{incident}} c^2}{21 \text{ MeV}} \right)^2 \quad (9)$$

to  $\gamma^{2/3}$ , since the formation zone increases with  $\gamma$  while the mean distance for the particle to scatter through an angle  $\theta_{\text{peak}} \approx \frac{1}{\gamma}$  is independent of  $\gamma$ .

#### Detectors

Most any detector that works in the energy region of 1-100 keV can be used when the transition radiation is separated from the particle track, including streamer chambers,<sup>5</sup> sodium iodide scintillators,<sup>6</sup> solid state detectors,<sup>6</sup> and proportional chambers.<sup>6,7</sup> With no separation, the detector must be thin, since the absolute magnitude of the Landau fluctuations increases with thickness. Thus far, gas proportional chambers have been used exclusively. Krypton and xenon (with 5-10 % CH<sub>4</sub>) are the best gasses because of their large photoelectric cross sections. In many cases the lower Z of krypton is compensated by its lower dE/dx and strategically located K edge (14 KeV). Its slight radioactivity (~ 500 Hz /liter)

normally causes no problems. Multiwire liquid xenon detectors now being developed<sup>11</sup> might have one additional useful property — sufficient resolution to separate the transition radiation from the particle track within a reasonable drift distance.

#### Some Experimental Results

Figure 3 shows results from a run in a 3 GeV/c beam at the Bevatron.<sup>7</sup> Sum counts from 11 multi-wire proportional chambers without radiators and electrons with a radiator set (100 - 1/2 mil (0.0005 inches) Mylar foils spaced 30 mils apart) placed in front of each chamber. The shift from pions to electrons without radiators is due to the relativistic rise in ionization energy loss. Electrons with and without an equivalent absorber (a single piece of 50 mil Mylar) give the same distribution, indicating, as expected, that bremsstrahlung is not important. A further rise, due to transition radiation is seen when radiator assemblies are placed in front of each chamber. 85% of the equivalent absorber events are below a discrimination threshold set near the cross over point; 85% of the radiator events are above the same threshold.

#### Uses

From work done so far, it is clear that a modest extension of present techniques (more chambers, slightly better radiators, more sophisticated treatment of the data) will permit the identification of particles with  $\gamma \geq 2000 - 3000$  at the several percent level, for example 400 GeV/c pions in the presence of 400 GeV/c K and p. The main advantages of transition radiation detectors, besides their usefulness at very high values of  $\gamma$ , lie in their wide angular acceptance (Cerenkov counters at NAL energies

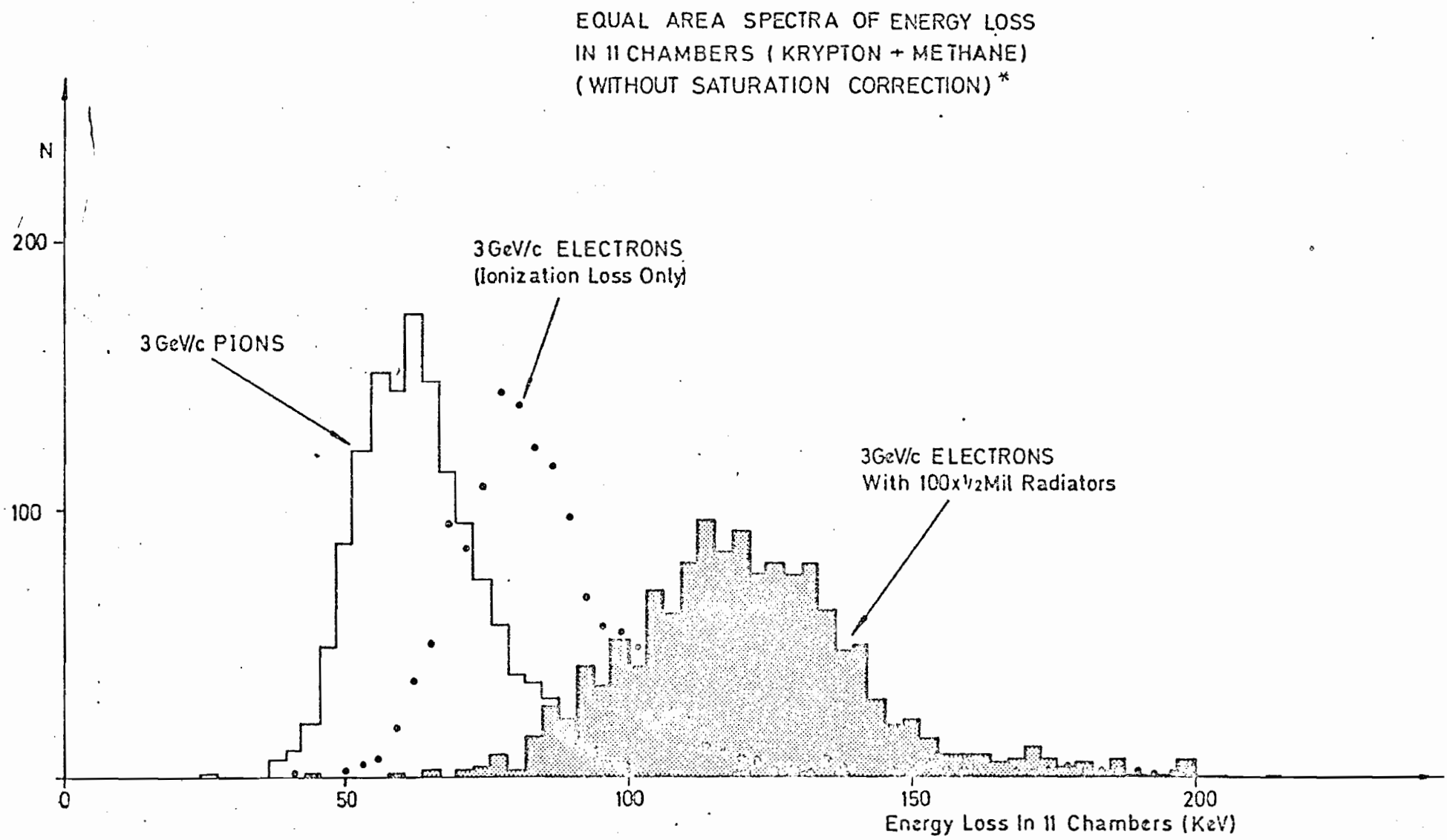


Fig. 3

\* Saturation in some of the readout channels causes a systematic underestimate of the number of large values.

typically limit at angles of  $\sim 10^{-3}$  to  $10^{-5}$  radians) and their potential ability to handle several simultaneous particles — both important in studying reaction products. These advantages are shared by particle identifiers using the relativistic rise in  $dE/dx$ , which should work up to  $\gamma$ 's of  $\sim 200$ . There still is a gap between 200 and 2000. Closing it with an effective, wide-angle detector remains a challenge for the future.

S. Parker  
U. of Hawaii  
Sept. 1972

#### References

1. V. L. Ginzburg and I. M. Frank, JETP 16, 15 (1946).
2. P. Goldsmith and J. V. Jelley, Phil. Mag 4, 836 (1959).
3. J. E. Lilienfeld, Physik. Zeit. 20, 280 (1919).
4. F. Bass and V. M. Yakovenko, Soviet Physics Uspekhi 8, 420 (1965); G. M. Garibian, Yerevan Preprint E<sup>W</sup>-10-13 (1970); G. M. Garibian, Adventures in Experimental Physics, α, 12D (1972). These papers contain extensive bibliographies.
5. A. I. Alikhanian, Adventures in Experimental Physics, α, 107 (1972) and earlier papers cited in Ref. 4.
6. C. L. Wang, G. F. Dell, Jr., H. Uto, and L. C. L. Yuan, Phys. Rev. Lett. 29, 814 (1972); H. Uto, L. C. L. Yuan, G. F. Dell, Jr., and C. L. Wang, Nucl. Instr. and Meth. 97, 389 (1971) and earlier papers cited there.
7. F. Harris, T. Katsura, S. I. Parker, V. Z. Peterson, R. Ellsworth, G. B. Yodh, W.W. M. Allison, C. B. Brooks, J. H. Cobb, and J. H. Mulvey, The Experimental Identification of Individual Particles by the Observation of Transition Radiation in the X-Ray Region, submitted to Nucl. Instr. and Meth.
8. D. Robbins and J. Mack, NASA Report TM X-58083 (1972); A minor typographical error has been corrected here. J. Docher, Phys. Rev. D 3, 2652 (1971).
9. G. M. Garibian and C. Yang, Soviet Physics JETP 34, 495 (1972); V. G. Baryshevskii and I. D. Feranchuk, Soviet Physics JETP 34, 502 (1972); A. I. Alikhanyan, G. M. Garibian, M. P. Lorikyan and K. K. Shikhlyarov, Soviet Physics JETP Letters 13, 142 (1971).
10. G. B. Yodh, private communication.
11. R. A. Muller, S. E. Derenzo, G. Smadja, D. E. Smith, R. G. Smits, H. Zaklad, and L. W. Alvarez, Phys. Rev. Lett. 27, 532 (1971).